LOWER OLIGOCENE CORALLINE ALGAE OF THE UROMIEH SECTION (QOM FORMATION, NW IRAN) AND THE OLDEST RECORD OF *TITANODERMA PUSTULATUM* (CORALLINOPHYCIDAE, RHODOPHYTA)

DANIELA BASSO[1], GIOVANNI COLETTI[1], VALENTINA ALICE BRACCHI[1] & MOHSEN YAZDI-MOGHADAM[2]

[1*]Univ. of Milano - Bicocca, Dept. of Earth and Environmental Sciences, P.za della Scienza 4, 20126 Milano, Italy
[2]National Iranian Oil Company Exploration Directorate, Sheikh Bahayi square, Seoul street,1994814695, Tehran, Iran

Abstract. The Rupelian Uromieh section of the Qom Formation was analyzed with the aim to provide a first description of its coralline algal assemblages, and benthic paleoenvironmental evolution through time. The presence of *Nummulites fichteli*, *Nummulites vascus*, *Halkyardia maxima* and *Subterraniphyllum thomasii*, together with the absence of *Nephrolepidina* and *Eulepidina* confirm an early to middle Rupelian age. In the lower part of the section, the abundance of miliolids and corals suggests a proximal inner-platform environment, while upsection the increase in large rotaliids, coralline algae and bryozoans points toward a distal inner-platform/proximal middle-platform setting. Coralline algal assemblages support this interpretation, with Sporolithales and Hapalidiales becoming more common in the upper part of the section. Within the coralline assemblage, *Lithoporella melobesioides* and *Titanoderma pustulatum* are two of the most common species, together with articulated coralline algae. *S. thomasii* is more common in coral-rich intervals, confirming that the distribution of this species was confined to shallow-water environments. The specimens of *T. pustulatum* recovered in the Uromieh section predate all the other known records of this species, indicating that the origin of *T. pustulatum* should be dated at least at the early Rupelian.

INTRODUCTION

Coralline algae are one of the most relevant carbonate producers in the photic zone of modern oceans (e.g. Basso 2012; Riosmena-Rodríguez 2017). They occur as binders stabilizing hermatypic coral reefs, produce autogenic bioconstructions (at both tropical and temperate latitudes), may form unattached free-living nodules (rhodoliths) and are able to colonize, with both crustose and articulated plants, almost any available hard substrate in the photic zone (Sanfilippo et al. 2011; Benzoni et al. 2011). They commonly occur in the shelf environment since the late Cretaceous and they are espe-

cially widespread in the Cenozoic (Bourrouilh Le Jan & Hottinger 1988; Halfar & Mutti 2005; Braga et al. 2010; Pomar et al. 2017). Coralline-algal limestones are actually so common that they represent an important economic resource, hosting various large hydrocarbon reservoirs (Sattler et al. 2004; Vaziri-Moghaddam et al. 2006; Pomar et al. 2015; Coletti et al. 2017). Notwithstanding this extremely wide distribution, most coralline algae are not very useful in stratigraphy and relatively underemployed in paleoecological reconstructions, because of the wide stratigraphic distribution of most species, their complex and sometimes confusing taxonomy and geographically uneven record.

The Qom Formation, one of the main reservoir in Iran (Yazdi-Moghadam 2011) is located at
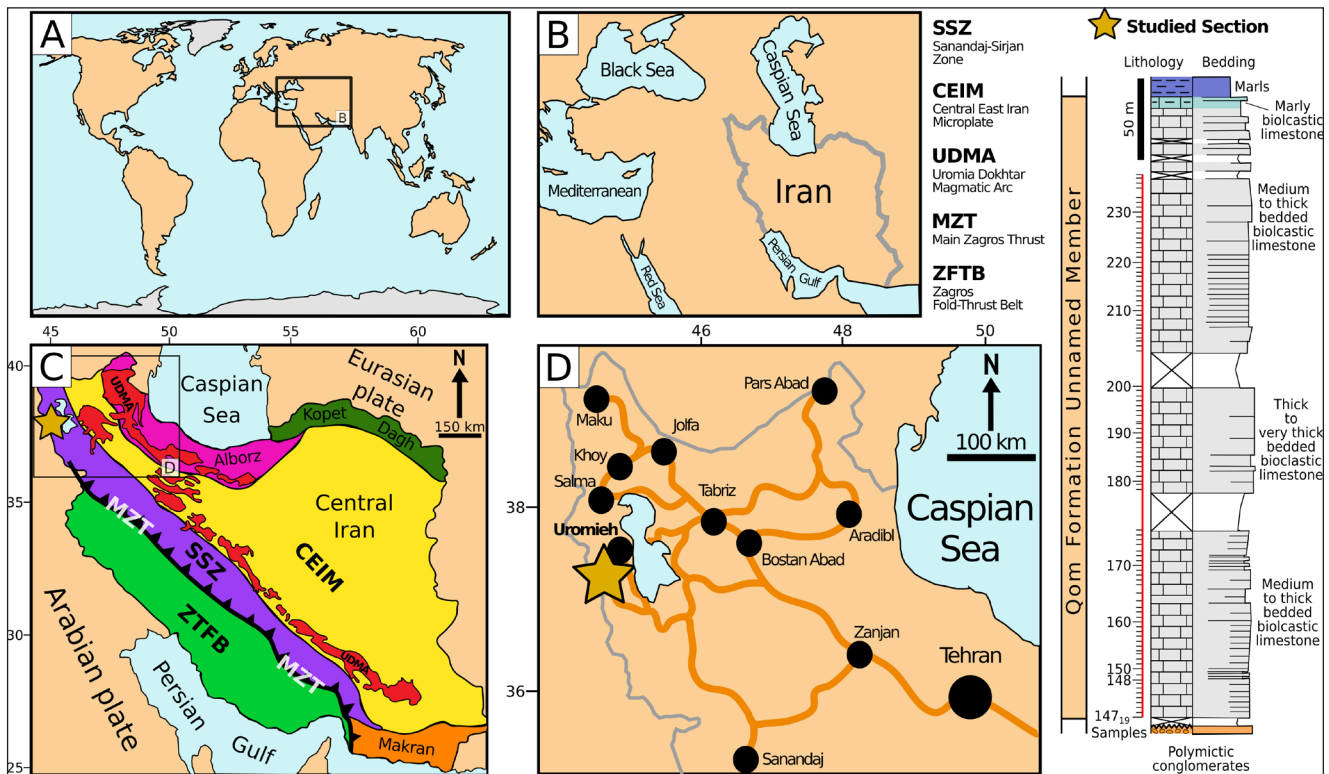
Fig. 1 - Study area and lithostratigraphic column of the Uromieh section; the red bar with sample numbers indicates the investigated interval. A-B) Location of the study area. C) Simplified geological map of Iran (modified after Agard et al. 2011) showing the main tectonic subdivisions and location of the studied section. D) Road map of the study area.

the bridge between the Tethyan and the Indo-Pacific region, a key area in a period during which the connection between the two bioprovinces was still active. Although a relatively well-established stratigraphic scheme of the Qom Formation is available (Reuter et al. 2009; Mohammadi et al. 2013, 2015; Yazdi-Moghadam et al. 2018) a taxonomic account and a paleoenvironmental analysis based on its calcareous red algae are presently lacking. The aim of this paper is to contribute to the knowledge of the shelf benthic associations recorded in the Rupelian of Iran, by shedding light on the stratigraphic distribution of calcareous red algae, as witness of biogeographically relevant past seaways and migrations.

GEOLOGICAL AND STRATIGRAPHIC SETTING

The Iranian plateau is a tectonically active region within the Alpine-Himalayan orogenic belt. It is composed of several structural units bounded by major faults and characterized by different sedimentary sequences, such as: Zagros fold and thrust belt, Sanandaj-Sirjan Zone (SSZ), Uromia-Dokhtar

Magmatic Arc (UDMA), Central Iran, Alborz, Kopet Dagh, and eastern Iran (e.g., Stöcklin 1968; Stöcklin & Nabavi 1973; Berberian & King 1981) (Fig. 1). Central Iran is separated from SSZ by the UDMA and exhibits complex structural features that are the result of a long geodynamic history from Paleozoic time up to the present (Letouzey & Rudkiewicz 2005; Zanchi et al. 2009, 2016; Zanchetta et al. 2013, 2018). Central Iran and the Zagros segment formed a single continental unit prior to Permian rifting and opening of the Neotethys Ocean. Following the subduction of the Neotethys, which started during the Late Triassic-Early Jurassic, the northward migration of the Arabian plate continued up to the continental collision with the Eurasian/Iranian plate during the Oligocene/Miocene (Berberian & King 1981; Davoudian et al. 2016). The UDMA is marked by intense and long-lasting magmatic activity that peaked during the Eocene (e.g., Bina et al. 1986; Agard et al. 2011; Hassanzadeh & Wernicke 2016). The SSZ includes Proterozoic and Cambrian magmatic rocks and Paleozoic sedimentary cover, but is mainly characterized by moderately metamorphosed rocks

Fig. 2 - Overview of the skeletal assemblages and facies of the Uromieh section, that correlates with the Unnamed Member of the Qom Formation at the type locality. From the left: the first column sketches the assemblage variation along with the change of relative dominance of different taxa (sample numbers and sample spacing on the marked left line). The second column includes the results of the visual estimation based on comparative tables. The third column presents examples of the distinct biofacies recorded in the section; number of representative sample in the upper left corner. The fourth column (on right) presents the distribution of the main biostratigraphic markers identified in the section. Legend for components on the bottom right.
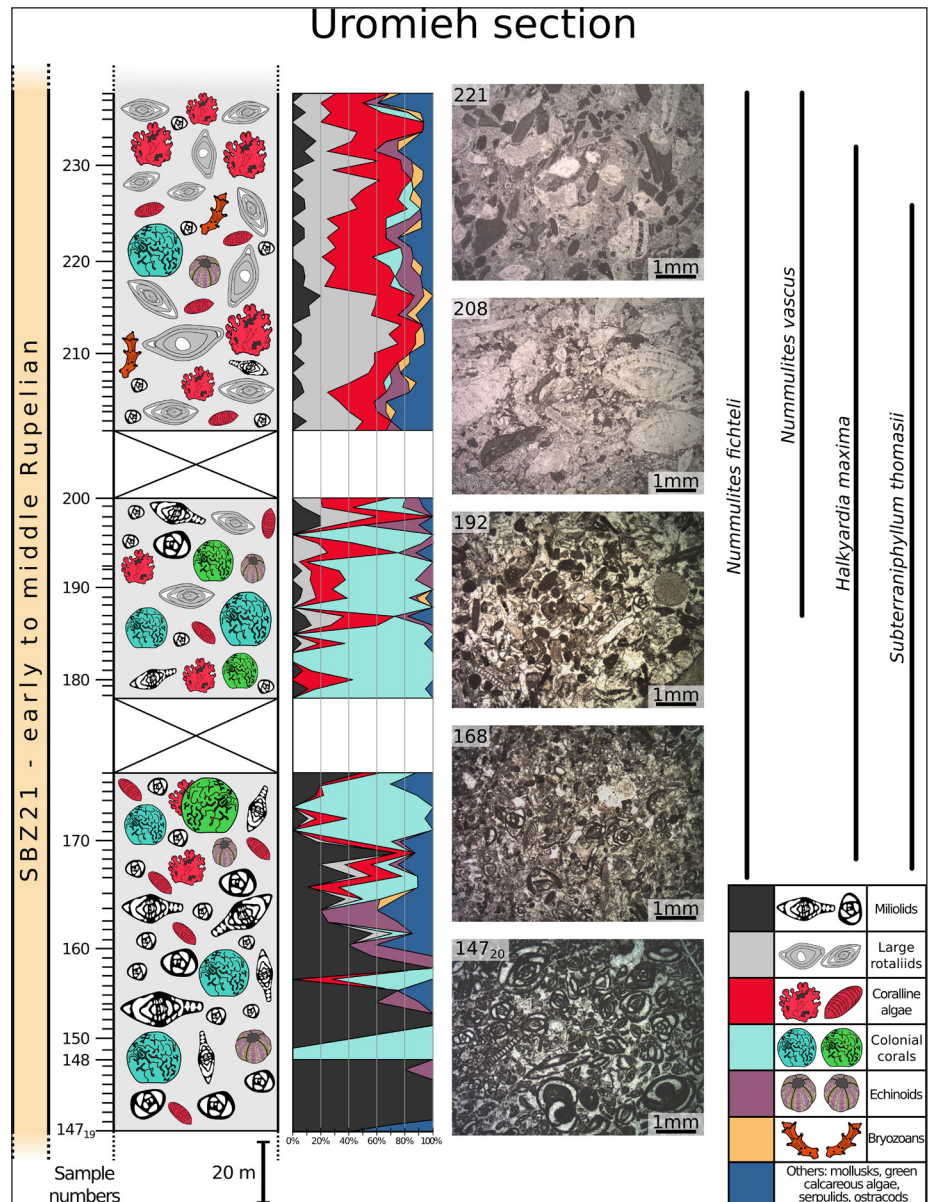
of Jurassic age unconformably overlain by shallow water orbitolinid-bearing limestones of Barremian-Aptian age (Stöcklin 1968; Hassanzadeh & Wernicke 2016). The Arabia-Eurasia collision caused the deformation of the SSZ, followed by the sedimentation of extensive Oligocene-Miocene marine deposits (Morley et al. 2009). The Lower Red Formation (Oligocene), the Qom Formation (lower Oligocene-middle Miocene), and the Upper Red Formation (Burdigalian-Tortonian) comprise the main stratigraphic units of the Central Iran Basin (Furrer & Soder 1955; Gansser 1955; Abaie et al. 1964; Ballato et al. 2008; Mattei et al. 2012). Furrer & Soder (1955) divided the Qom Formation into six members, including: basal limestones, sandy marlstones, alternating marlstones and limestones, evaporites, green marlstones, and top limestones. Bozorgnia (1965) recognized the shallow marine *Nummulites*-bearing carbonates in the central part of the basin, far from the Qom area, and considered these lower Oligocene strata, that he called "Unnamed Member", as a part of the Qom Formation. The investigated Uromieh area belongs to the Sanandaj-Sirjan Zone (Fig. 1) and the studied section of the Qom Formation consists of *Nummulites*-bearing limestones that overlay thick polymictic conglomerates and are overlaid by marlstones rich in planktonic foraminifera (Fig. 1; Yazdi-Moghadam 2011). Due to their composition, the examined limestones can be lithologically correlated with the Unnamed Member of the Qom Formation (sensu Bozorgnia 1965).
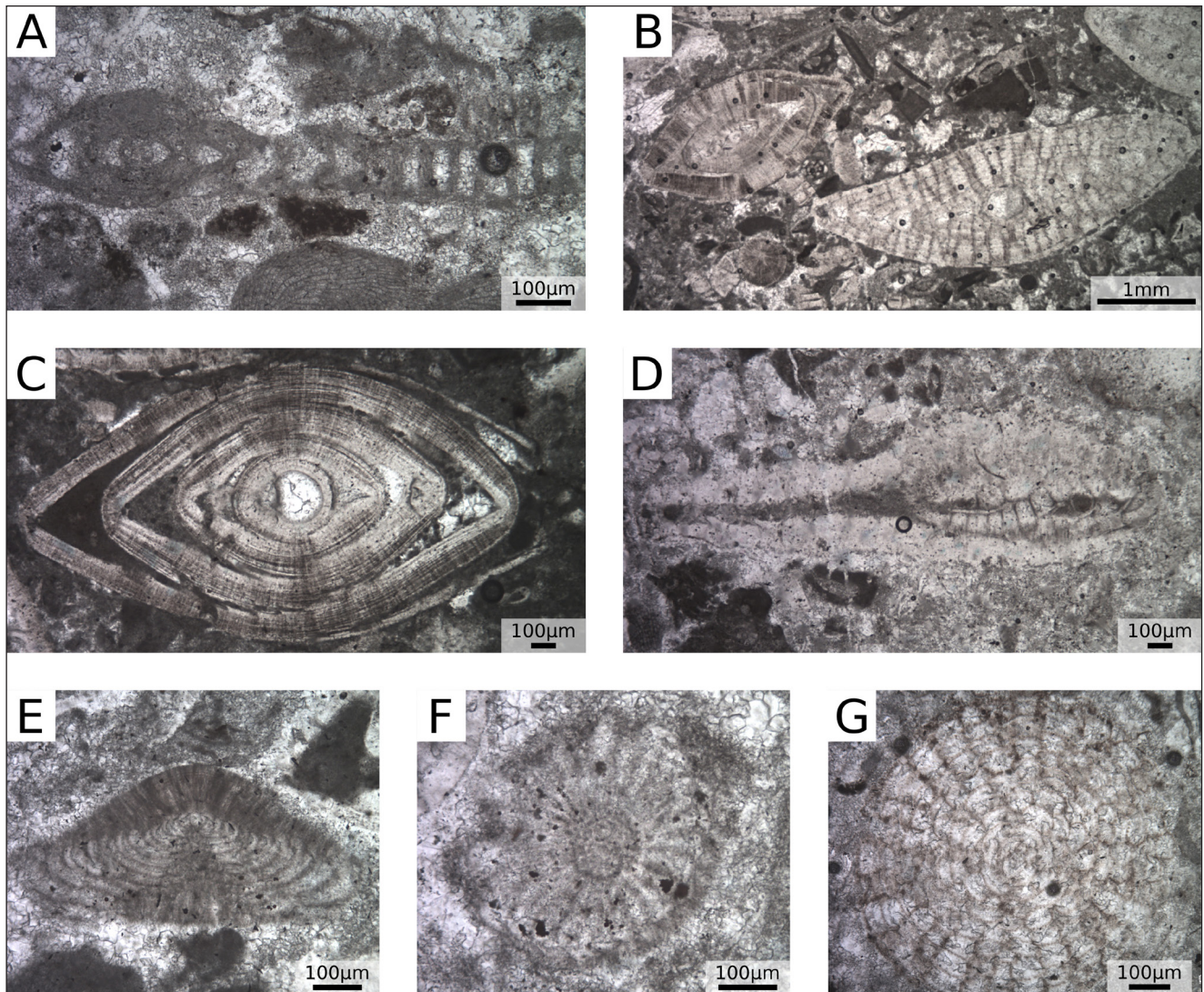
Fig. 3 - Benthic foraminifera of the Uromieh section. A) *Peneroplis*; sample 168. B) *Nummulites vascus* (left) and *Nummulites fichteli* (right); sample 227. C) *Nummulites vascus*; sample 211. D) *Heterostegina*; sample 209. E) *Halkyardia maxima*, axial section; sample 219. F) *Halkyardia maxima*, cross-section parallel to the base; sample 232. G) *Sphaerogypsina*; sample 166.

MATERIAL AND METHODS

The study is based on the analysis of 130 thin sections of samples collected south of the city of Uromieh in northwestern Iran (coordinates of the base of the section: Lat 37°20′35.4″ N, Long 44°56′15.6″ E). The semi-quantification of the skeletal grains was based on visual estimation (Baccelle & Bosellini 1965; Flügel 2010) of the main carbonate components: miliolids, large rotaliids, coralline algae, colonial corals, echinoids, bryozoans. The less common components (mollusks, green calcareous algae, serpulids and ostracods) have been grouped into the category *other skeletal grains*. The available material was not containing a sufficient amount of corallines to justify their point-count quantification. Therefore, we only reported the occurrence of the recognizable red calcareous algae along a sketch of the stratigraphic section. The generic classification of foraminifera follows Loeblich & Tappan (1987), Hottinger et al. (1991) and Hottinger (2007). Coralline algae growth-form terminology follows Woelkerling et al. (1993). The terminology for the vegetative anatomy of fossil crustose taxa follows Hrabovský et al. (2015), using hypothallus and perithallus as synonyms for ventral core of basal filaments and peripheral zone, respectively, as widely used in early and modern phycological literature (among the most recent contributions: Caragnano et al 2016; Hernandez-Kantun et al. 2016; Richards & Fredericq 2018; Pezzolesi et al 2019). The features of the vegetative thallus were observed along longitudinal radial sections (Quaranta et al. 2007; Vannucci et al. 2008). The diameter of cells was measured including their wall; cell length was measured as the distance between two primary pit connections and includes the cell wall (Basso et al. 1996). The vegetative and reproductive features of coralline algae were described and measured following Basso et al. (1996), Quaranta et al. (2007) and Vannucci et al. (2008). Higher rank coralline-algal taxonomy follows Woelkerling (1988), later modified by Harvey et al. (2003), Le Gall et al. (2009), Nelson et al. (2015), and Rösler et al. (2016). Adaptation to the paleontological use follows Braga et al. (1993) and Hrabovský et al. (2015). At genus level, the separation of *Phymatolithon* from *Lithothamnion* in the fossil is based on the morphological features highlighted by Basso (1995) and in particular on the shape of epithallial cells and relative length of subepithallial initials (which are as short as or shorter than underlying cells in *Phymatolithon*, while are as long as or longer in *Lithothamnion*). Diagnostic characters for species circumscription within the genus *Sporolithon* follow Maneveldt et al. (2017).
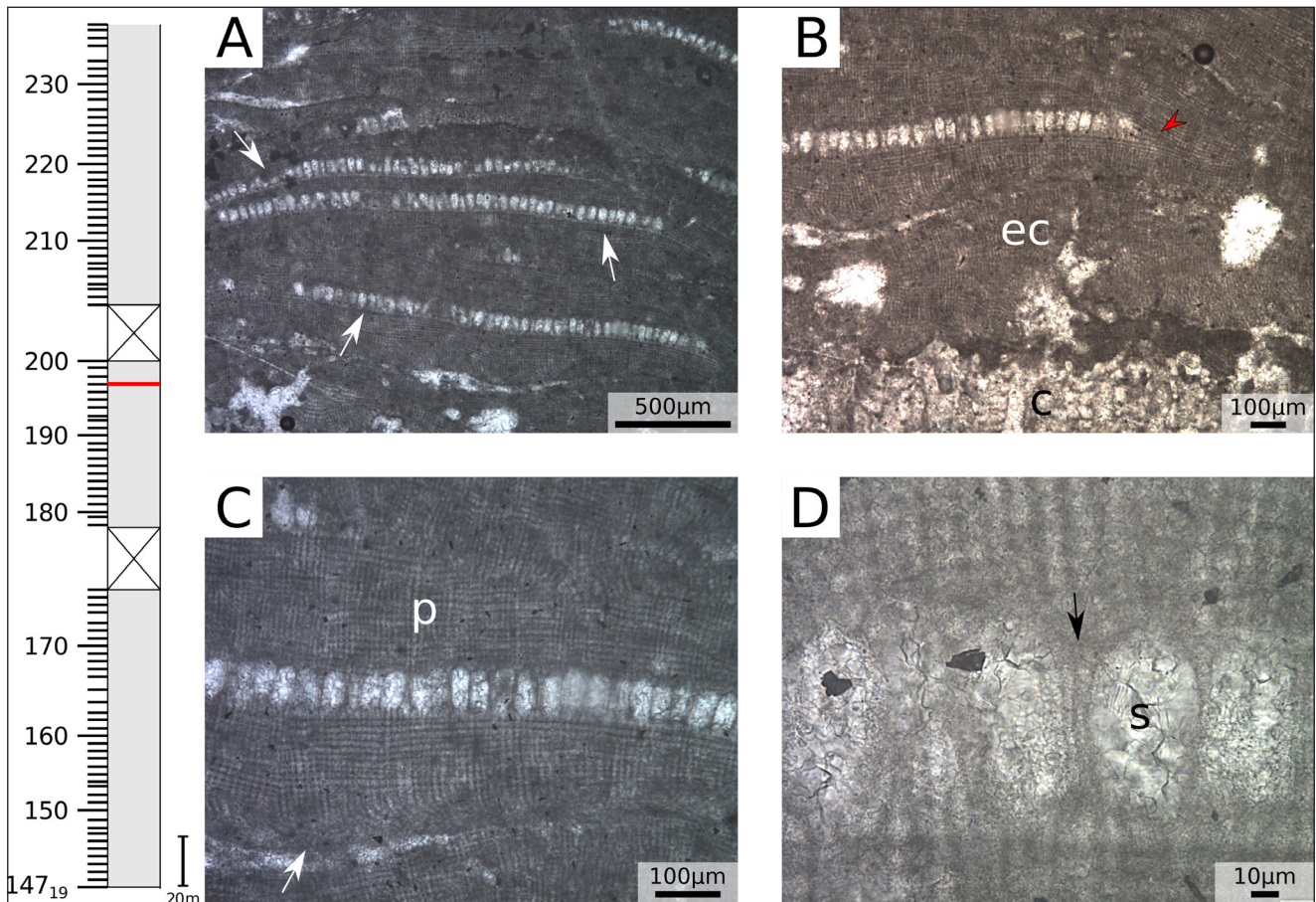
Fig. 4 - *Sporolithon airoldii* (Fravega) Vannucci, Quaranta, Basso, 2010. A) Sample 197. The fertile thallus shows three superposed sori (arrows), originally slightly raised above the surrounding thallus surface. B) Detail of the monomerous structure and the overgrown coral (c) and encrusting coralline (ec). Red arrowhead to show the sorus originally raised above the surrounding thallus surface. C) Thin non-coaxial hypothallus (arrow); grid-like perithallus (p), and one sorus composed of a single layer of numerous elliptical sporangial compartments. D) Four sporangial compartments (s) separated by sterile paraphyses (arrows).

RESULTS

Benthic foraminifera (mainly miliolids and large rotaliids), hermatypic corals and coralline algae dominate the Uromieh section, accompanied by less common echinoids and bryozoans. Other skeletal grains like mollusks, green calcareous algae, serpulids and ostracods are rarer (Fig. 2).

Benthic foraminifera

Miliolids (including *Triloculina*, *Penarchaias*, *Peneroplis*, *Dendritina* and *Borelis*; Fig. 3A) dominate the benthic foraminiferal assemblage from sample 147 to sample 184. Large rotaliids become increasingly more common and clearly dominate from sample 201 upward. The association includes *Nummulites fichteli* Michelotti, 1841 (sample 166 upward; Figs 2, 3B), *Nummulites vascus* Joly & Leymerie, 1848 (sample 187 upward; Figs 2, 3C), *Halkyardia maxima*

Cimerman, 1969 (samples 168 to 232; Figs 2, 3E-F), *Heterostegina* (sample 169 upward; Fig. 3D), *Operculina* (sample 158 upward), *Victoriella* (samples 184 to 225), *Neorotalia* (sample 150 upward) and Asterigerinoidea (sample 165 upward). *Sphaerogypsina* (Fig. 3G) and *Planorbulina* are also present but they are less abundant. Agglutinated foraminifera are present in most samples; the encrusting agglutinated *Haddonia* is often present growing over coral fragments.

Coralline algae

Division **RHODOPHYTA** Wettstein, 1901
Class **FLORIDEOPHYCIDAE** Cronquist, 1960
Subclass **CORALLINOPHYCIDAE** Le Gall
& Saunders, 2007
Order **Sporolithales** Le Gall & Saunders, 2009
Family Sporolithaceae Verheij, 1993
Genus *Sporolithon* Heydrich, 1897

Sporolithon airoldii (Fravega) Vannucci, Quaranta & Basso, 2010
Fig. 4

Description. Thallus encrusting, about 500 µm in thickness, with monomerous construction (Fig. 4A-C). Cell filaments composed of small square cells, 6 to 11 µm in diameter and 9 to 13 µm in length, both in the hypothallus and in the perithallus. The hypothallus is 50-95 µm thick and non-coaxial (Fig. 4C). The perithallus has a very regular, grid-like appearance. Cell fusions are present. Trichocytes not observed. Sporangial compartments grouped into large sori, each one with tens of compartments, whose surface is raised 4-5 cells (about 60 µm) above the surrounding vegetative surface (Fig. 4 A-C). The sporangial compartments are elliptical in shape, 25 to 45 µm in diameter and 60 to 80 µm in height. The compartments are very close and may appear in contact or mostly separated by one or two sterile filaments (paraphyses, Fig. 4D). The cells composing the paraphyses are longer than those of the perithallus and about half their diameter. Row of elongated cells at the base of the sporangial compartments absent. The sporangial compartment floors is flush with the surrounding vegetative surface. Remnants of stalk cells can be observed within the sporangial compartments (Fig. 4C).

Remarks. During the Paleogene, the genus *Sporolithon* was a common element of the Tethyan coralline algal flora (among others: Braga & Bassi 2007; Basso et al. 2009; Brandano et al. 2010; Quaranta et al. 2012; Coletti et al. 2016). Most of the described Oligocene Tethyan species are characterized by large, rectangular, often remarkably elongated vegetative cells (e.g. Vannucci et al. 2000a; Bassi & Nebelsick 2000; Misra et al. 2001; Gale 2009; Aguirre et al. 2011). On the contrary, the species *S. airoldii* is very distinctive for its particularly small square cells and short sporangial compartments (Vannucci et al. 2010a). The studied specimen of *Sporolithon* perfectly matches the description of the holotype (Vannucci et al. 2010a).

Distribution. This species is uncommon, occurring in the middle part of the section (sample 197), where it encrusts a coral fragment and overgrows another unidentified, very thin encrusting coralline. The stratigraphic distribution of *S. airoldii* ranges from the lower Rupelian to the Burdigalian-Serravallian of the western Tethys (Vannucci et al 2010a).

Sporolithon sp. 1
Fig. 5

Description. Encrusting to warty-fruticose growth-form (Fig. 5A). Monomerous construction with a ventral core up to 130 µm thick. The hypothallus is mostly non-coaxial, but hypothallial cells locally show a synchronous division, resulting in an imperfect coaxial organization (Johansen 1981; Fig. 5B). Hypothallial cells are rectangular and elongated, 8 to 14 µm in diameter and 11 to 19 µm in length. The perithallus shows patches of regularly arranged, grid-like, well-aligned cells, passing to local wavy appearance and poor cell alignment, due to rectangular cells of variable size 10 to 14 µm in diameter and 12 to 21 µm in length (Fig. 5B). Cell fusions are present. Trichocytes not observed. Tens of sporangial compartments are grouped in very large sori, with their surface raised of about 3-4 cells (50-80 µm) above the surrounding vegetative surface (Fig. 5A, C), and with their base flush or slightly sunken (1 cell) below the surrounding vegetative surface. Sporangial compartments are quite slender and elliptical in shape, 35 to 55 µm in diameter and 80 to 120 µm in height. The compartments are separated by a variable number of paraphyses (mostly 2 to 3, up to 6), each one formed by 2-3 cells much longer than those of the surrounding perithallus. Stalk cells were not observed within the compartments. Row of elongated cells at the base of the sorus not observed (Fig. 5D).

Remarks. This species differs from *S. airoldii* in having much larger vegetative cells and sporangial compartments. Several living and fossil species have been described within the genus, but the diagnostic morphological characters for their circumscription are still poorly defined, while most fossil species require a revision within a modern systematic approach (Hrabovský et al. 2015). For these reasons and in consideration of the paucity of the available material we leave the species in open nomenclature.

Distribution. *Sporolithon* sp. 1 occurs in the uppermost part of the section (Sample 234, Fig. 5), attached to hard substrates (micritized bioclasts, bryozoan colonies, encrusting thalli of other coralline algae and Peyssonneliales).
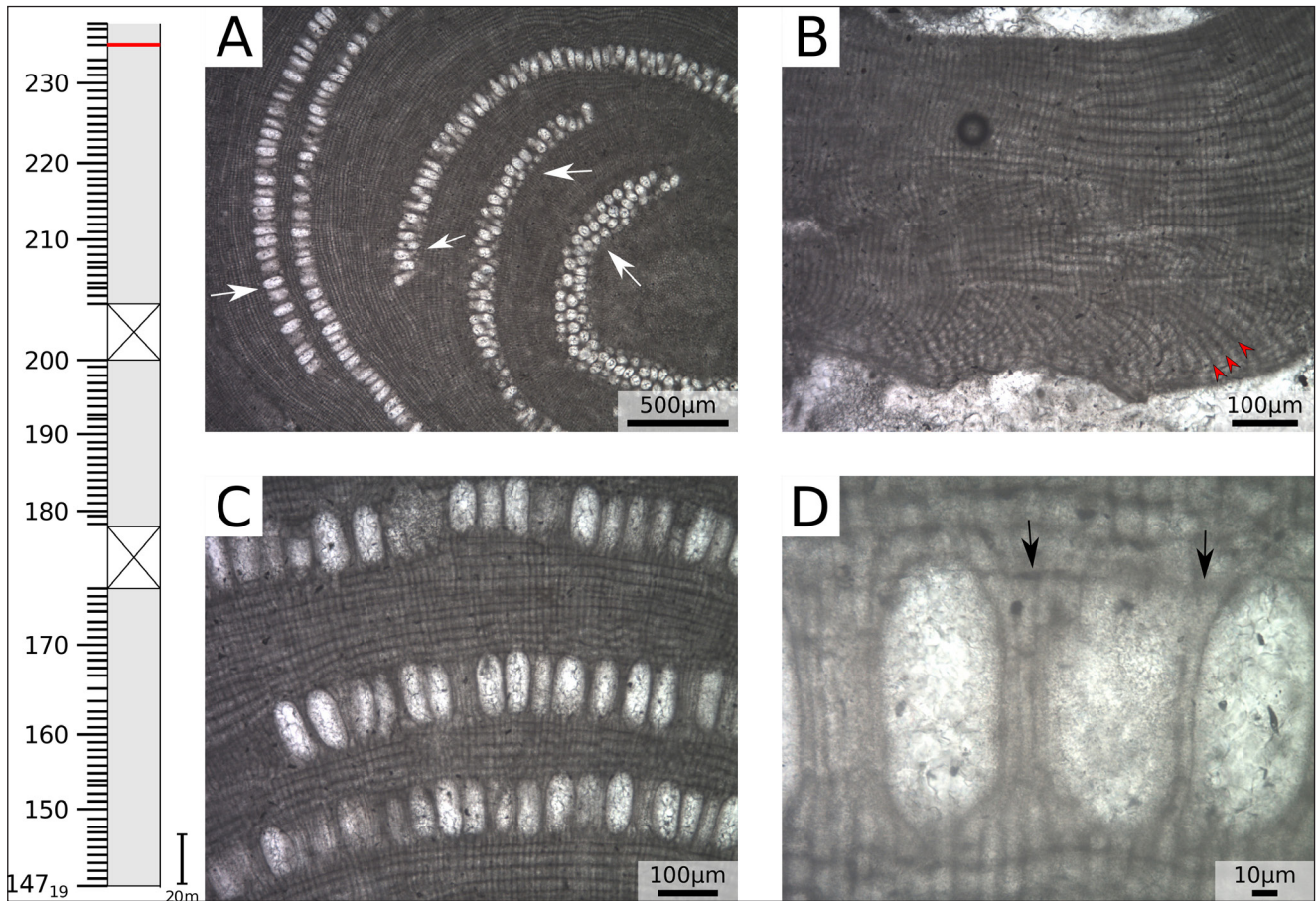
Fig. 5 - *Sporolithon* sp. 1. A) Sample 234. A fertile protuberance with several generations of sori buried in the thallus (arrows). B) Monomerous construction. The synchronous division of the hypothallial cell filaments results in an incomplete, local coaxial arrangement (red arrowheads). Note the variable length of the perithallial cells of adjacent filaments. C) A magnification of three sori. D) A detail of three sporangial compartments showing the elongate cells in paraphyses (arrows) and absence of elongated cells at the base of compartments.

Sporolithon sp. 2
Fig. 6

Description. Thallus encrusting to fruticose, with a monomerous construction (Fig. 6A). Non-coaxial plumose hypothallus up to 190 μm thick, giving rise toward the thallus surface to the perithallial filaments (Fig. 6A, B). Perithallial cells rectangular, with very variable length in adjacent filaments and within the same filament (8 to 12 μm in diameter and 10 to 24 μm in length) (Fig. 6D). Sporangial compartments isolated or grouped in sori, each compartment about 100 μm high and 50-57 μm in diameter, but mostly obliquely cut, thus preventing a precise measurement and the detection of the shape of the cells at the base of the sporangial compartments (Fig. 6C). One specimen showed the same vegetative anatomy and the occurrence of both isolated sporangial compartments and gametangial conceptacle chambers in the same plant. Gametangial conceptacles buried in a protuberance were pear-shaped, about 50 to 100 μm in diameter and 50 to 120 μm high (Fig. 6D).

Remarks. The co-occurrence of gametangial and sporangial conceptacles in the same *Sporolithon* plant was described by Verheij (1993) and reported for the first time in the fossil by Hrabovský et al. (2015) for *Sporolithon lvovicum* (Maslov). The observed features of the vegetative and reproductive anatomy of *Sporolithon* sp. 2 are compatible with the original description of *S. lvovicum* provided by Bassi et al. (2007). However, given the scarcity and incompleteness of our material we keep the taxonomy in open nomenclature. The sporangial plant and the sporangial/gametangial plant occur in different beds of the upper part of the succession (Fig. 6), therefore their conspecificity, although supported by the anatomical evidence, must be considered with caution.
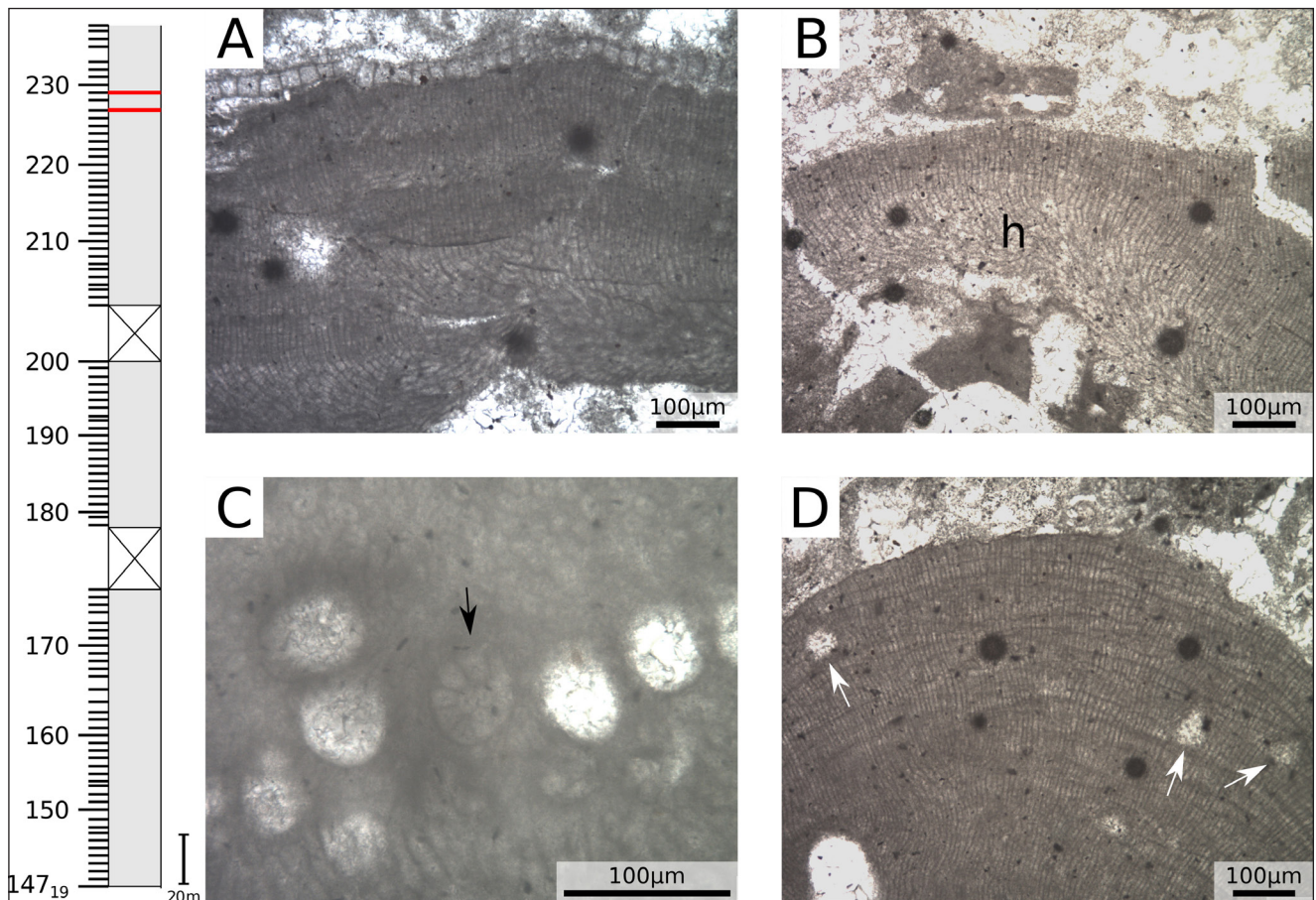
Fig. 6 - *Sporolithon* sp. 2. A) Sample 229. Monomerous construction. Note the thick plumose hypothallus, with cells bending upward and downward, on bottom right; the plumose organization is not visible on the left. B) Sample 229. Thick hypothallus with the same transition from plumose to non plumose (h). C) Sample 229. Sporangial compartments in oblique section, tangential on the one in the centre of the figure (arrow), where the geometry of nine cap cells at the top of the sporangial compartment is visible (arrow). Note the transversally cut vegetative cells on the top. D) Sample 227. Longitudinal section of three gametangial conceptacles (arrows). The two gametangial conceptacles on right have the typical pear-shaped outline, as reported in several species of the genus *Sporolithon*.

Distribution. The sporangial thallus of *Sporolithon* sp. 2 occurs in the upper part of the section (Sample 229, Fig. 6), attached to solid substrates (micritized bioclasts, bryozoan colonies, encrusting thalli of other coralline algae and Peyssonneliales). The gametangial/sporangial thallus was observed in sample 227.

Order **Hapalidiales** Nelson, Sutherland, Farr & Yoon, 2015
Family Hapalidiaceae Gray, 1864
Subfamily Melobesioideae Bizzozero, 1885
Genus *Lithothamnion* Heydrich, 1897

Lithothamnion* cf. *giammarinoi Fravega, Piazza & Vannucci, 1993
Fig. 7

Description. Thallus encrusting, less than 500 μm thick. Monomerous organization with mostly thin (about 50 μm or less) non-coaxial to plumose ventral core, up to a maximum thickness of 100 μm (Fig. 7A). Hypothallial cells rectangular and elongated, 7 to 10 μm in diameter and 13 to 18 μm in length. Perithallus composed of small sub-square cells 8 to 12 μm in diameter and 8 to 12 μm in length. Cell fusions are present in both the hypothallus and the perithallus. Sporangial multiporate conceptacles elliptical in longitudinal section (LS). The conceptacle chambers are 475 to 700 μm in diameter and 185 to 210 μm in height. The roof of the conceptacle is convex, about 50 μm thick, composed of filaments less than 10 cells long. Pore canals are cone-shaped, about 25 μm in diameter at their proximal end, and tapering toward the surface of the conceptacle (Fig. 7B).

Remarks. Due to the taphonomic overprint, it was not possible to identify the shape of the epithallial cells, though preserved at the thallus surface by the encrustation from other organisms. However, the subepithallial initials appear longer than the underlying cells. This observation allows a confident placement in the genus *Lithothamnion*. The other observed vegetative and reproductive features are compatible with those of the holotype of *L. giammarinoi* (Fravega et al. 1993; Coletti 2016).

Distribution. *L.* cf. *giammarinoi* occurs in the middle part of the section (Sample 184; Fig. 7). The observed specimen grew over a coral fragment.

Order **Corallinales** Silva & Johansen, 1986
Family Corallinaceae Lamouroux, 1812
Genus *Subterraniphyllum* Elliot, 1957

Subterraniphyllum thomasii Elliot, 1957

Fig. 8

Description. Thallus composed of calcified intergenicula (Vannucci et al. 2000b), up to 2 mm in length and 500 µm in diameter. Some intergenicula show dichotomous branching (Fig. 8A). Each intergeniculum is formed of a central large-celled medulla and a peripheral small-celled cortex (Fig. 8B-D). The medulla is organized in horizontal layers composed of very large, polygonal, elongated cells, 30 to 70 µm in diameter and 50 to 110 µm in length. Lateral fusions are very common in the medulla. The medullary cells become significantly smaller and shorter toward the periphery of intergeniculum, where they form the cortex (Fig. 8 C-D). The cortex is composed of relatively small rectangular cells, elongated in LS. Cell fusions are common in the cortex (Fig. 8 C-D). Reproductive structures, as reported by Vannucci et al. (2000b) were not observed.

Remarks. This species was originally described as a geniculate taxon, and later treated as such by most authors (Elliott 1957; Johnson 1966; Mastrorilli 1968; Lemoine 1977; Poignant 1985). Bassi et al (2000), based on the absence of preserved genicula and the occurrence of thallus branching, concluded that *S. thomasii* was not "segmented" and was a non-geniculate taxon. However: 1) some geniculate coralline algal species possess both branched segments (= bifurcating intergenic-
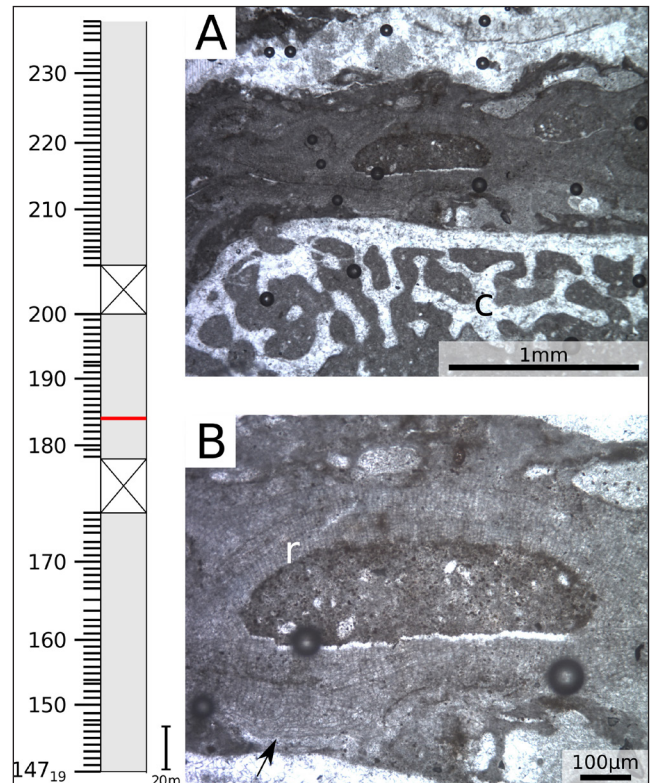

Fig. 7 - *Lithothamnion* cf. *giammarinoi* Fravega, Piazza & Vannucci, 1993. A) Sample 184. A fertile thallus encrusting another coralline and a coral (c). B) Magnification of A) to show the monomerous construction, the thin non-coaxial hypothallus (arrow), and the multiporate roof (r) of the conceptacle chamber, protruding over the surrounding thallus surface.

ula) and genicula (for example, species of *Amphiroa* Lamouroux (Harvey et al. 2013) and *Corallina* Linnaeus (Johansen 1981)) therefore, thallus bifurcation and occurrence of genicula are not mutually exclusive in coralline algae; 2) genicula are seldom preserved in fossil material (Bassi et al. 2000, and references therein); 3) Vannucci et al. (2000b) described for the first time the reproductive anatomy of *Subterraniphyllum* and some obviously articulated thalli, with derivative intergenicula connected with the parent intergenicula by a tapering end. Therefore, we consider *S. thomasii* as a geniculate taxon.

Distribution. *S. thomasii* is common in the studied section, especially between samples 189 and 205 and between samples 217 and 226 (Fig. 8). The observed intergenicula are always isolated, however, the very distinctive vegetative anatomy of this coralline leaves no doubt about its identification. Published reports of this species span the late Eocene to the early Miocene (Aquitanian), with common reports from the Oligocene (Mastrorilli 1968; Bassi et al. 2000; Vannucci et al. 2000b). However,
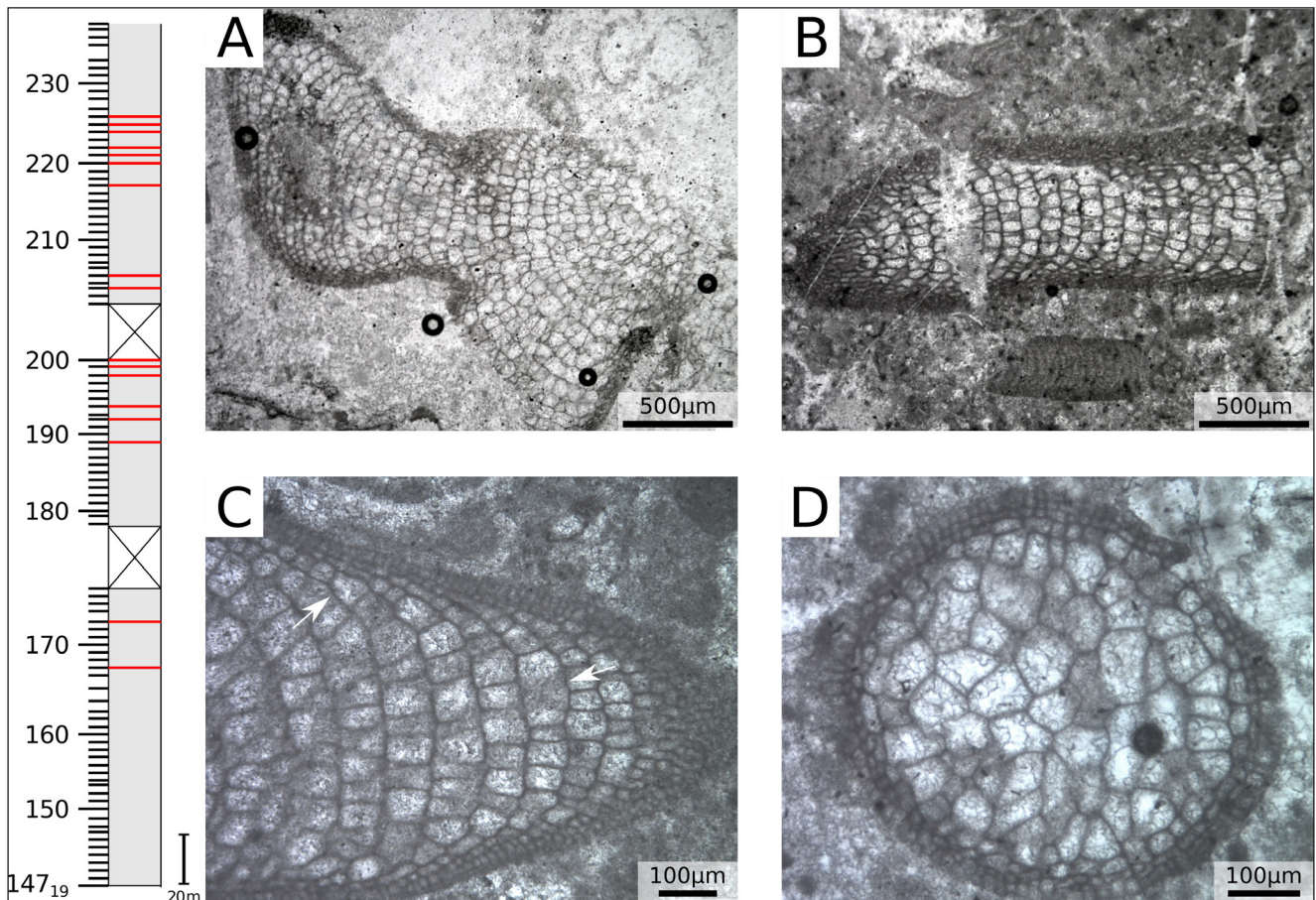
Fig. 8 - *Subterraniphyllum thomasii* Elliott. A) Sample 225. An intergeniculum showing dichotomous branching. B) Sample 167. The large polygonal medullary cells sharply decreasing in size toward the periphery of the intergeniculum to form a small-celled cortex. C) Sample 192. Cortical cell organization and numerous cell fusions (arrows) in longitudinal (C) and radial (D) section.

the Miocene and Eocene reports are biostratigraphically poorly constrained by the associated large foraminiferal assemblage, or not supported by adequate illustrations, and cannot be verified. Therefore, in agreement with Cahuzac & Poignant (1997) and Bassi et al. (2000), the stratigraphic distribution of *S. thomasii* is reliably limited to the Oligocene.

Subfamily Lithophylloideae Setchell, 1943
Genus *Titanoderma* Nägeli, 1858

***Titanoderma pustulatum*** (J.V. Lamouroux)
Nägeli, 1858

Fig. 9

Description. Encrusting thallus of variable thickness, from very thin and composed of few cells, up to about 1 mm and >8 cells thick (Fig. 9A). Several thalli may be superimposed within each crustose specimen (Fig. 9C). Dimerous construction, with hypothallus composed of a single layer of palisade cells 32-70 µm high and up to 29 µm wide (Fig. 9B). Perithallus characterized by palisade cells slightly smaller than those of the hypothallus, 10 to 25 µm in diameter and 23 to 58 µm in length. Cell fusions not observed. Trichocytes not observed. Presumed asexuate conceptacles are raised above the surrounding thallus surface (Fig. 9C-D). They are uniporate and flask shaped, with a conceptacle chamber 370 to 525 µm in diameter and 110 to 175 µm high, with flat floor laying 2-3 cells below the thallus surface. Pore canal conical with a basal diameter of 110 to 120 µm and a length of 85 to 120 µm. The apical end of some pores is flared. The roof is composed of 2 to 5 celled-filaments. The cells at the base of the conceptacle chambers are generally shorter than those subtending them, in the vegetative part of the perithallus (Fig. 9C-D).

Distribution. Among the non-endophytic species belonging to the genus *Titanoderma*, this species is distinctive because of the unique combination of growth-form, shape and size of the

Fig. 9 - *Titanoderma pustulatum* (J.V. Lamouroux) Nägeli, 1858. A) Sample 180. Thick specimen composed of several fertile thalli (red arrowheads), bearing many uniporate conceptacles with flat floor (arrows). B) Thallus showing dimerous construction, completely formed by palisade cells, larger in the monostromatic hypothallus (arrows). C) and D) Magnification of the vegetative, palisade cells. Note the lack of cell fusions and the occurrence of the typical, obliquely-cut epithallial cell (black arrow). E) and F) Detail of two uniporate conceptacles originally raised above the surrounding thallus surface, with floor 3 cells below the surrounding thallus surface (white numbers) and roof formed of filaments protruding into the pore canal (black arrowheads). Note superimposed thalli (red arrowheads).
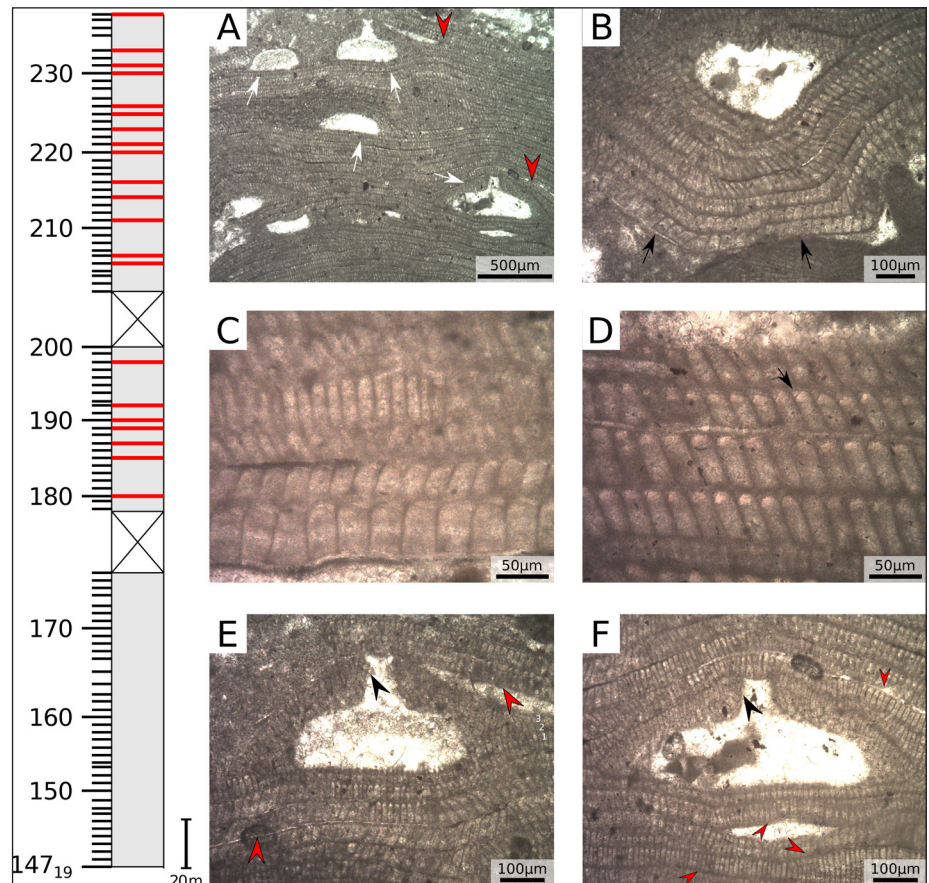
sporangial conceptacle chamber and pore canal, depth of the conceptacle chamber floor relative to the surrounding thallus surface, number of cells layers forming the roof of the conceptacles, thallus thickness (Chamberlain & Irvine 1994; Harvey et al. 2009; Van der Merwe & Maneveldt 2015). A large specimen of *T. pustulatum* occurs in sample 180, in the lower half of the section, encrusting a coral. Small fragments of *T. pustulatum* occur in most samples (Fig. 9). Based on these results, the presumed origin of this cosmopolitan living species (Guiry & Guiry 2019) must be moved back to the early Rupelian.

Subfamily Mastophoroideae Setchell, 1943
Genus *Lithoporella* Foslie, 1909

Lithoporella melobesioides Foslie, 1909
Fig. 10

Description. Thin encrusting thallus with dimerous construction. Applanate branches are commonly superposed in several layers (Fig. 10A). Hypothallus composed of large rectangular cells, 12 to 34 μm in diameter and 25 to 40 μm in height,
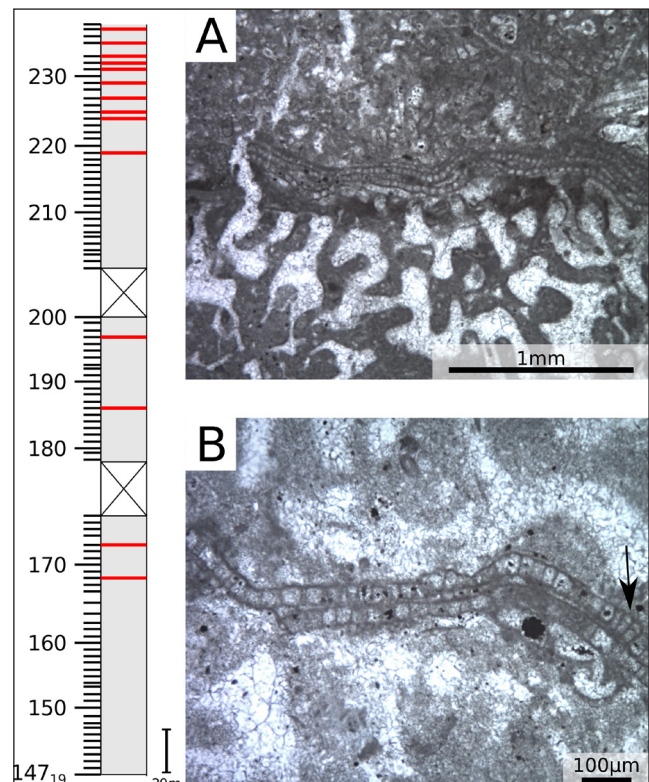

Fig. 10 - *Lithoporella melobesioides* Foslie, 1909. A) Sample 173. A thin thallus overgrowing a coral. B) Detail of A) to show the square cells each one terminating with a small epithallial cell (arrow).
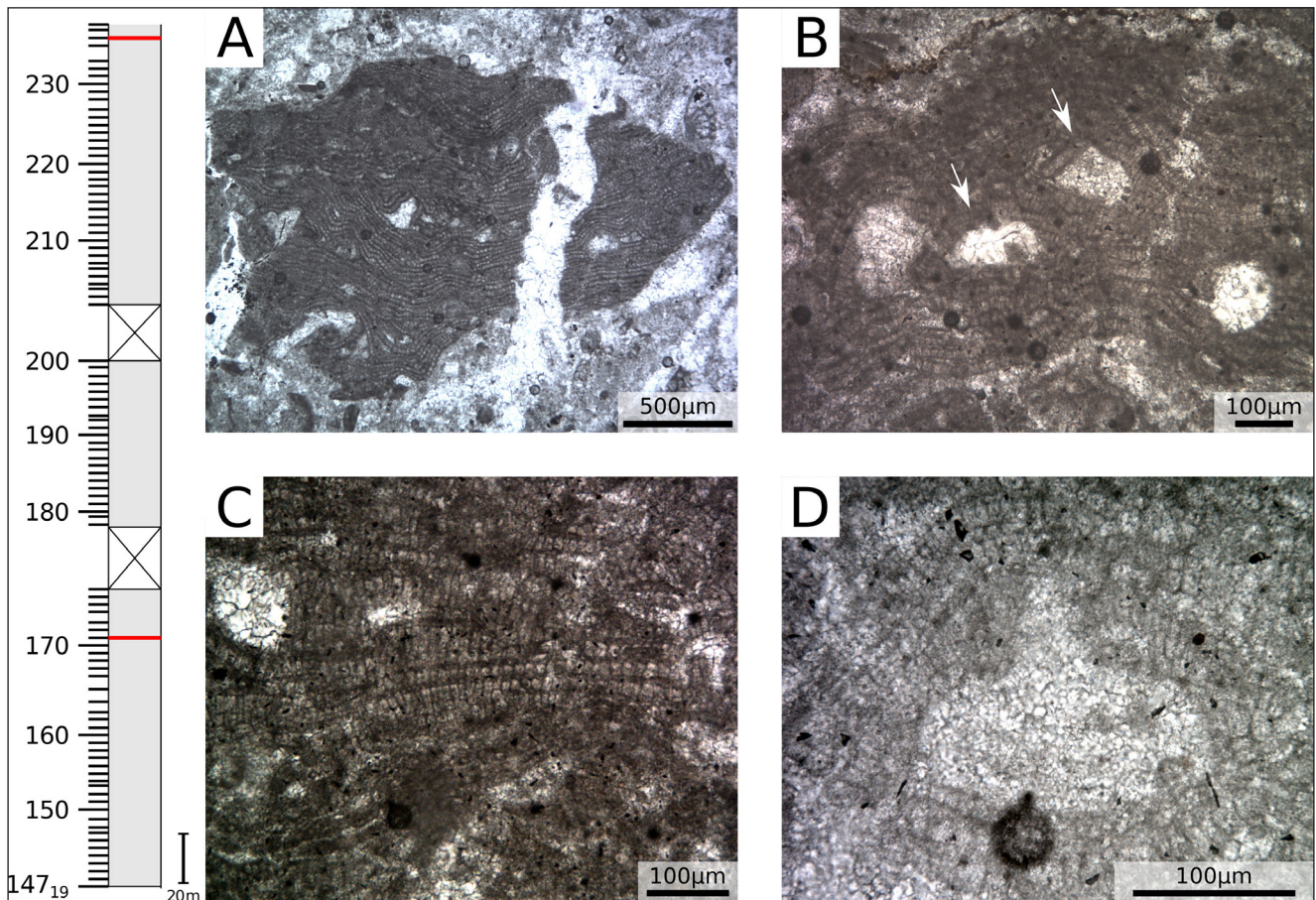
Fig. 11 - *Lithoporella minus* Johnson, 1964. A) Sample 171. A well-developed thallus formed by several applanate branches. B) Sample 235. Uniporate conceptacles in a fertile thallus (arrows). C) Sample 235. Thallus showing dimerous construction. Note epithallial cells over each basal cell. D) Sample 235. Uniporate conceptacle originally protruding over the thallus surface.

commonly connected by cell fusions (Fig. 10B). Ep-ithallial cells dome-shaped, 20 to 25 µm in diameter and 10 to 13 µm in height. In most cases, only the hypothallus is present.

Distribution. Relatively thick crusts, grow-ing over corals and created by a large number of thalli stacked together, occur in samples 173, 225 and 229 (Fig. 10). Smaller crusts and fragments oc-cur in most of the samples.

Lithoporella minus Johnson, 1964
Fig. 11

Description. Thin encrusting thallus with dimerous construction. A single layer of non-pal-isade cells mostly 9-12 µm in diameter and 8-20 µm long, connected by cell fusions, form applanate branches overgrowing one another (Fig. 11A-C). A single epithallial cell terminates each cell filament at the thallus surface. A thin perithallus is developed

only encasing a uniporate conceptacle (Fig. 11D), which has a chamber 181 µm in diameter and 143 µm high, including the conical pore-canal.

Distribution. A well-developed thallus oc-curs in sample 171bis (Fig. 11).

Remarks. It has been suggested that *Lithoporella melobesioides* could be conspecific with either *Porolithon improcerum* (Foslie & M. Howe) M. Howe, 1920 (Penrose in Womersley 1996; Harvey et al. 2006) or with a *Mastophora* species (Keats et al. 2009). In the fossil record, based on the small-er cells, *Lithoporella minus*, rather than *Lithoporella melobesioides*, appears to be more closely related to *Porolithon improcerum*. The structure of the observed conceptacle roof (Fig. 11D), however, recalls the anatomical organization of the genus *Mastophora* Decaisne (Caragnano et al. 2018).

Subfamily Neogoniolithoideae Kato & M. Baba, 2011
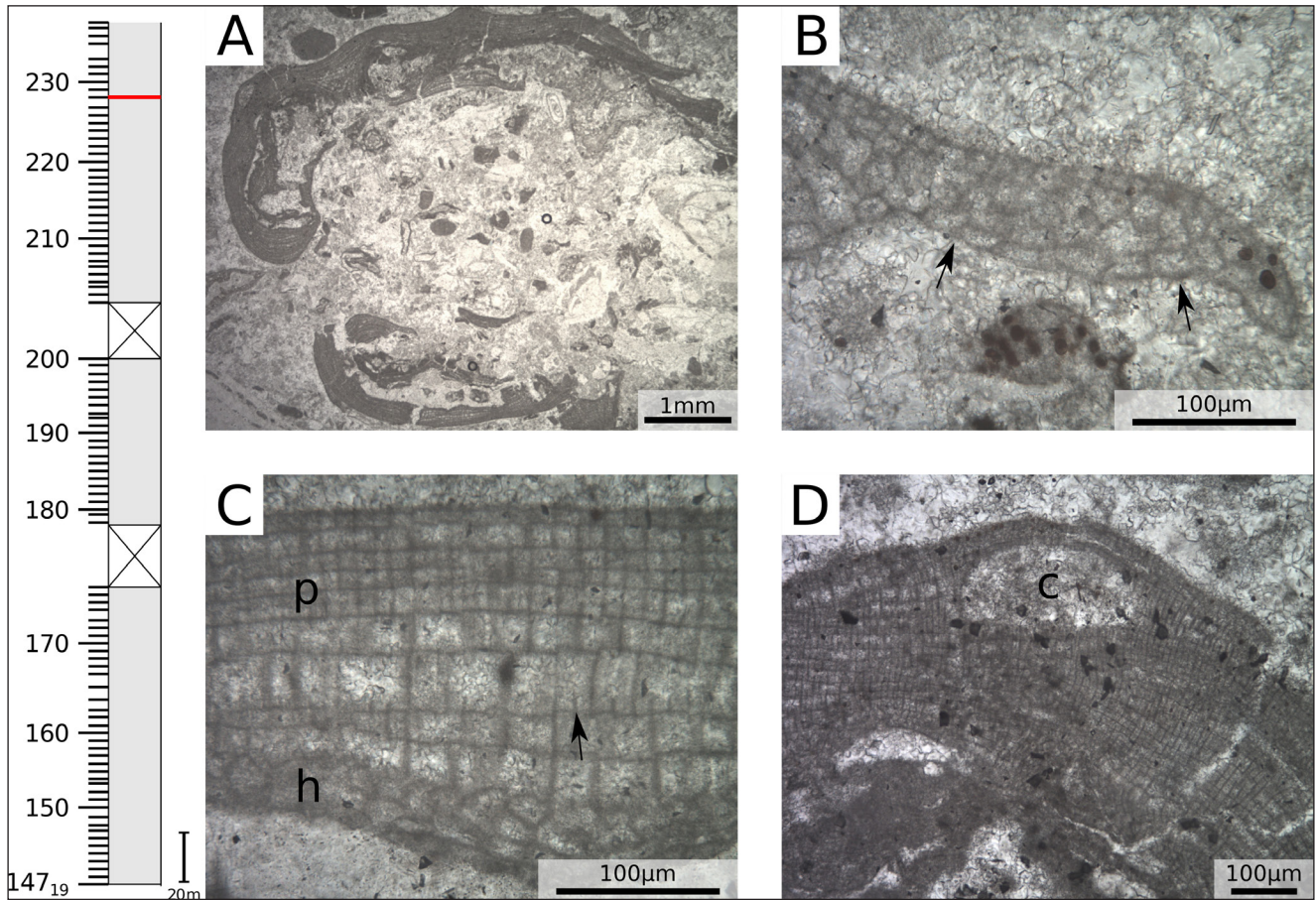emended Rösler et al., 2016

Fig. 12 - *Spongites* sp. A) Sample 228. A hook-shaped, fertile thallus. B) Magnification of the growing margin of a thallus with monomerous construction, showing a ventral filament of cells (hypothallus; arrows) dividing and bending toward the thallus surface. C) Sample 228. Detail of the monomerous construction, thin non-coaxial hypothallus (h) and perithallus (p) with large cell fusions (arrow). D) Fertile thallus with a presumed uniporate conceptacle chamber (c) with flat floor.

Genus *Spongites* Kützing, 1841

Spongites sp. 1
Fig. 12

Description. Thin encrusting thallus (about 100 to 200 μm thick) with monomerous construction (Fig. 12A-C). Non-coaxial hypothallus composed of few filaments of large polygonal cells (Fig. 12B-C). Perithallus composed of elongated rectangular cells 7 to 13 μm in diameter and 13 to 28 μm in height. Adjacent perithallial filaments connected by common cell fusions (Fig. 12C). Trichocytes not observed. The few observed conceptacles are incomplete and small, with internal cavities 250 to 270 μm in diameter and 105 to 115 μm in height (Fig. 12D).

Distribution. The specimen occurs in sample 228 (Fig. 12), growing around different skeletal grains. The hooked form of the crusts suggests an epiphytic lifestyle.

Other coralline algae. Poorly preserved and/or fragmentary thalli lacking diagnostic characteristics for species identification are present in most of the section. Some of the specimens can be included in the order Corallinales (samples 179, 189, 215, 227). Among the material that preserves some diagnostic characters, we observed a fragmentary but fertile specimen (Sample 227, Fig. 13A) about 100 μm thick (up to 250 μm in correspondence of the raised uniporate conceptacle). The conceptacle chamber is about 200 μm in diameter and 106 μm high, including the pore canal. The roof filaments are oriented parallel to the pore canal (Fig. 13A). The thallus has dimerous construction, cell fusions, and sparse trichocytes. These characters collectively point to a species of *Hydrolithon*, and possibly to *H. lemoinei* (Miranda) Aguirre et al. known from Oligocene to Badenian (Aguirre et al. 2011; Hrabovský et al. 2015; Chelaru & Bucur 2016).

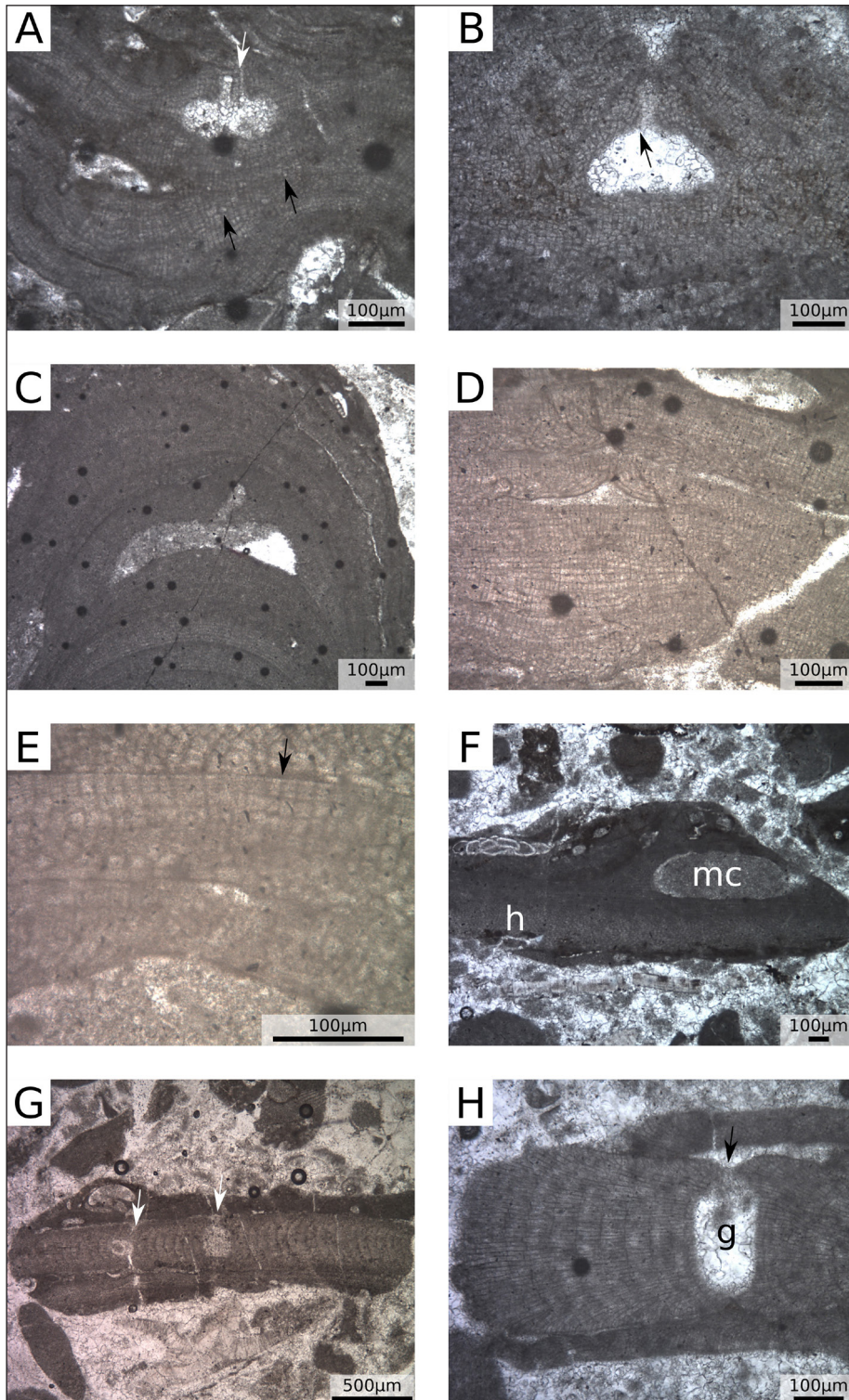Another specimen (sample 215) has a thin di-

Fig. 13 - Coralline algae of uncertain taxonomic position. A) Sample 227. ? *Hydrolithon lemoinei* (Miranda) Aguirre et al. Thallus with dimerous construction, uniporate conceptacle chamber with roof filaments parallel to the pore canal (white arrow). Note sparse trichocytes (black arrows). B) Sample 215. Chamberlainoideae ind. Note the thin dimerous thallus and the uniporate conceptacle chamber with roof formed by filaments running obliquely to the pore canal (arrow). C) Sample 233. ? *Spongites* cf. *personatus* (Airoldi) Vannucci et al. A fertile monomerous thallus with a large and asymmetric uniporate conceptacle chamber. D) Thin hypothallus and monomerous construction in superposed thalli of ? *Spongites* cf. *personatus*. E) Detail of hypothallus and flattened epithallial cells (arrows) of ? *Spongites* cf. *personatus*. F) Sample 189. Non-coaxial hypothallus (h) and multiporate conceptacle chamber (mc) in Hapalidiaceae ind. (sample 189). G), H), Sample 219. Common fragments of geniculate corallines. Note the thin encrusting non-geniculate corallines preventing the detachment of the two intergenicula (arrows) after the decomposition of the genicula (empty space=g).

merous thallus with a hooked shape, up to about 110 µm thick, composed of cell filaments connected by cell fusions. It bears a uniporate conical conceptacle protruding above the surrounding vegetative surface, whose chamber is 259 µm in diameter and 235 µm high, including the pore canal. The roof is composed of 4-6 celled filaments running obliquely to the pore canal (Fig. 13B). Trichocytes not observed.

The presence of cell fusions exclude any affinity with the Lithophylloideae. The dimerous thallus excludes the possibility that it could represent a *Neogoniolithon* plant or a gametangial plant of most Hapalidiales. On the base of the observed features, a placement of this probably epiphytic species in the newly erected subfamily Chamberlainoideae Caragnano, Foetisch, Maneveldt & Payri cannot be

ruled out (Caragnano et al. 2018) however, we are not able to achieve any confident identification.

Although incompletely preserved, a specimen in sample 233 shows a large and asymmetric uniporate conceptacle chamber, about 1 mm in diameter (Fig. 13C), a non-coaxial hypothallus (Fig. 13D), flattened to rounded epithallial cells (Fig. 13E), and the absence of trichocytes, that collectively allow to speculate its correspondence with ? *Spongites* cf. *personatus* (Airoldi) Vannucci, Quaranta & Basso (2008).

Other specimens likely belong to the order Hapalidiales (samples 189, 209, 225, 227, 229, Fig. 13F). Most of the observed specimens grew over coral fragments; others grew over large bioclasts or over the sediment. Articulated coralline algae are abundant and common in most of the samples, particularly from sample 167 onward (Fig. 13G-H).

Subclass **Rhodymeniophycidae** G.W. Saunders & Hommersand, 2004

Order **Peyssonneliales** Krayesky, Fredericq & J.N. Norris, 2009

Family Peyssonneliaceae Denizot, 1968

Genus *Polystrata* Heydrich, 1905

Polystrata alba (Pfender) Denizot, 1968

Fig. 14

Description. Thin thalli (100 to 200 μm) with foliose growth-form (Fig. 14A). Several thalli are irregularly superposed, each one composed of a central monostromatic mesothallus of large, square to polygonal cells, from which the perithallial cell filaments (= postigenous filaments in Bassi 1997) develop above (upper perithallus) and below (lower perithallus) (Denizot 1968; Kato et al. 2006). Perithallial filaments are composed of cells of decreasing diameter toward the thallus surface (Fig. 14B). The cells of each perithallial filament are connected by primary pit connections. No reproductive structures observed.

Distribution. *P. alba* occurs throughout the section, from sample 148 to sample 234 (Fig. 14). It is particularly abundant at the nucleus of a rhodolith in sample 234. The observed specimens grew on various bioclasts, micrite, and encrusting coralline algae. The record of *Polystrata* ranges from Early Cretaceous to Present (Rasser 2001). Among
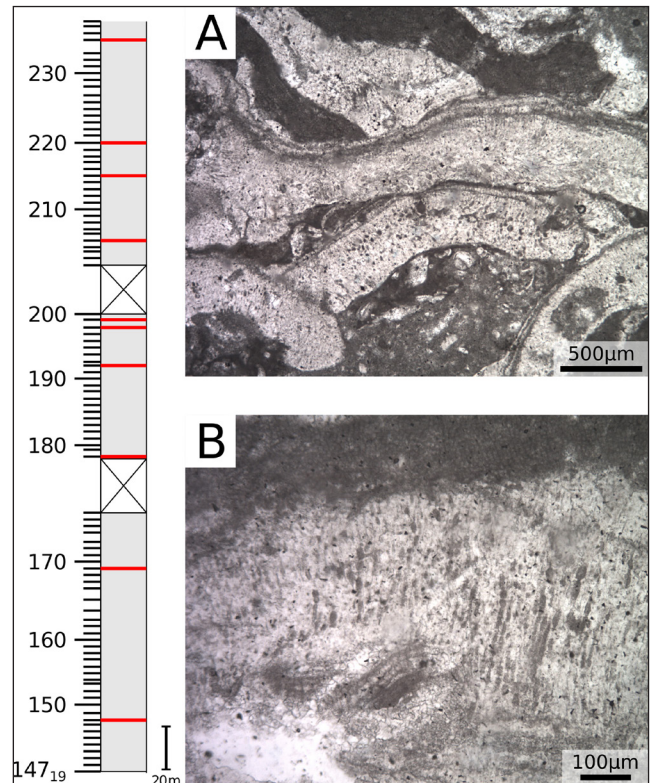

Fig. 14 - *Polystrata alba* (Pfender) Denizot, 1968. A) Superposed thalli in sample 234. B) Detail of cell filaments.

the living species, *Polystrata fosliei* (Weber van Bosse) Denizot is morphologically the closest to *P. alba* (Kato et al. 2006). The geographic distribution of *P. fosliei* includes the tropical and subtropical Atlantic and Pacific Oceans, and the Mediterranean Sea (Guiry & Guiry 2019).

BIOFACIES

Based on the dominant components, it is possible to identify the following skeletal assemblages along the section:

Miliolid facies

The lowermost part of the section (samples from 147_{19} to 160) is characterized by grainstones-packstones largely dominated by a diverse assemblage of porcellanaceous foraminifera (e.g. sample 147_{20}; Fig, 2) including *Dendritina* cf. *rangi*, *Austrotrillina* spp., *Spirolina* sp., *Triloculina trigonula* (Lamarck), *Triloculina* spp., and *Peneroplis thomasi* Henson. Corals are also locally common, while large rotaliids and small fragments of coralline algae are very rare. *P. alba* is the only calcareous alga identified in this interval with a single occurrence (Fig. 15).
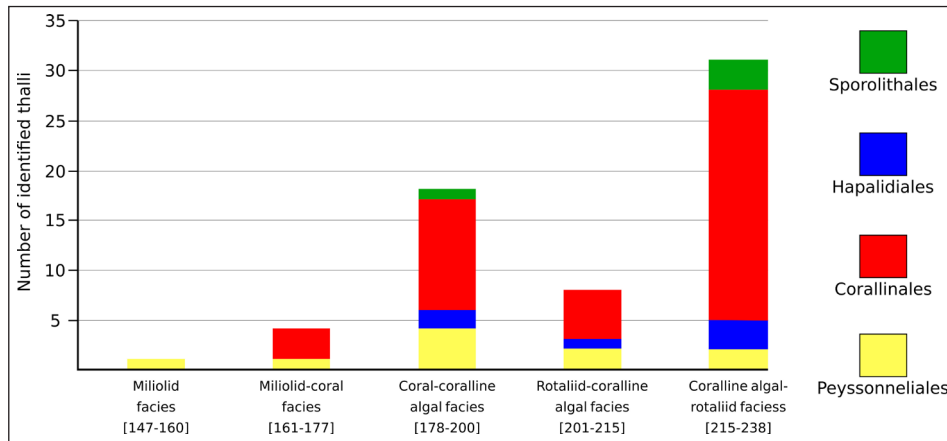
Fig. 15 - Bar plots summarizing the occurrences of red calcareous algae (non geniculate coralline algae and Peyssonneliales) in the five biofacies. Numbers in square brackets refer to the sample numbers as in Fig. 2.

Miliolid-coral facies

From sample 161 to 177 the microfacies consists of wackestones to grainstones. Porcellanaceous foraminifera are still abundant (e.g. sample 168; Fig. 2) and include the same assemblage as described for the Miliolid facies, with the addition of *Praerhapydionina delicata* Henson and *Penarchaias glynnjonesi* (Henson). Hermatypic corals become much more common and often dominate the skeletal assemblage (in particular between sample 167 and sample 177). Coralline algae, large rotaliids and echinoids also occur in this interval. The calcareous red algal association is composed of rare *P. alba, S. thomasii, L. melobesioides* and *L. minus* (Fig. 15).

Coral-coralline algal facies

Further upward (samples from 178 to 200) the microfacies consists of a packstones-grainstones characterized by a coral-dominated skeletal assemblage. Coralline algae and large rotaliids are significantly more common, while miliolids are less abundant (e.g. sample 192; Fig, 2). In this facies and in the Rotaliid-coralline algal facies upsection, the hyaline foraminifera reach their maximum diversity with several species of nummulitids (*Nummulites* spp, *Heterostegina* sp., *Operculina* sp.); echinoids also occur. The algal assemblage is rather diversified, and composed of *P.alba, S. thomasi, T. pustulatum, L. melobesioides, S. airoldii, L. giammarinoi* and other unidentified Hapalidiales (Fig. 15).

Rotaliid-coralline algal facies

The samples 201 to 215 consist of a packstones-grainstones with large rotaliids dominating the skeletal assemblage, together with subordinate coralline algae (e.g. sample 208; Fig. 2). Corals and miliolids are remarkably less common than in the Coral-coralline algal facies; echinoids and bryozoans are also present. The coralline association is composed of *S. thomasi, T. pustulatum* and some fragmented thalli of Hapalidiales ind. (Fig. 15).

Coralline algal-rotaliid facies

Upsection (samples from 215 to 238) the microfacies consists of packstones dominated by coralline algae, that occur as fragments (e.g. sample 221; Fig. 2) and rare, small rhodoliths. Large rotaliids are subordinate and, toward the top of this interval, *Victoriella* and *Halkyardia maxima* disappear. Miliolids, corals, echinoids and bryozoans are minor components of the assemblage (Fig. 2). The coralline algal assemblage is composed of *S. thomasii, T. pustulatum, L. melobesioides, L. minus* and *Spongites* sp. 1 (Fig. 15), associated with an increase in Hapalidiales and Sporolithales (*Sporolithon* sp. 1, *Sporolithon* sp. 2). Scattered occurrences of *P. alba* are also recorded.

DISCUSSION

Biostratigraphy

N. fichteli, N. vascus and *H. maxima*, together with the absence of either *Nephrolepidina* and *Eulepidina*, place the studied samples of Uromieh in the biozone SB 21 of Cahuzac and Poignant (1997), corresponding to early to middle Rupelian age (Zones O1 and O2 of Wade et al. 2011) (Fig. 2). This interpretation is also supported by several regional biostratigraphic schemes (Racey 1994; Jones & Racey 1994). The common presence of *S. thomasii*, one of the few coralline algae used in biostratigraphy, also points to an Oligocene age for the studied interval (Mastrorilli 1968; Sartorio & Venturini 1988; Bassi et al. 2000; Vannucci et al. 2000b; Vannucci et al. 2010b). Finally, the marlstones overlying the studied interval are placed in the biozone P20 of Spezzaferri (1994), corresponding to a late Rupelian age, due

the occurrence of *Turborotalia ampliapertura* (Bolli, 1957), *Globigerina praebulloides* Blow, 1959, *Globigerina tripartita* Koch, 1926, *Paragloborotalia nana* (Bolli, 1957), *Subbotina yeguaensis* (Weinzierl & Applin, 1929) and of *Chiloguembelina cubensis* (Palmer, 1934) (Yazdi-Moghadam 2011). This further supports an early to middle Rupelian age for the studied interval of the Uromieh section.

Coralline algae and paleoenvironmental interpretation

The section presents a general deepening upward trend (Fig. 2). This is testified by the change from a benthic foraminiferal assemblage dominated by shallow-water miliolids to one dominated by large-rotaliids, decreasing hermatypic corals and increasing coralline algae and bryozoans (Fig. 2; Montaggioni et al. 1986; Nebelsick et al. 2005, 2013; Basso et al. 2006; Brandano et al. 2009; Pomar et al. 2015, 2017). The presence of marlstones overlying the investigated interval further supports this interpretation (Fig. 1; Yazdi-Moghadam 2011).

Crustose Corallinales and articulated coralline algae, including *Subterraniphyllum*, dominate the coralline algal assemblage along the whole Uromieh section (Fig. 15). From the base of the section up to the top of the Miliolid-coral facies (sample 177) Corallinales largely dominate the assemblage (Fig. 15), while Hapalidiales and Sporolithales appear in the Coral-coralline algal facies (sample 178 to 200). Further upward, Sporolithales and Hapalidiales become more common (Fig. 15). Peyssonneliales occur in the whole section, although never dominant (Figs 2-4, 15). The increased coralline diversity, along with the observed changes in coralline association, are coherent with the variations in the invertebrate assemblage (decrease in miliolids and hermatypic corals and increase in large rotaliids), suggesting a change from a proximal inner-platform setting for the lower part of the section (from the base to sample 200) to a distal inner platform/proximal middle-platform for the upper part of the section (from sample 201 upward, Fig. 15; Adey 1979, 1986; Adey & Macintyre 1973; Adey et al. 1982; Minnery et al. 1985; Vadas & Steneck 1988; Perrin et al. 1995; Bassi 1997; Lund et al. 2000; Braga & Aguirre 2001; Braga et al. 2009; Coletti et al. 2018).

The observed distribution of *S. thomasii* provides useful information on the paleoecology of this species. In the Uromieh section, *S. thomasii* is mainly associated with *Lithoporella* and *T. pustulatum*, other articulated coralline algae, and hermatypic corals. The evidence from the studied succession, therefore, is in substantial agreement with previous studies (Bassi & Nebelsick 2000; Vannucci et al. 2000b; Vannucci et al. 2010b), reporting *S. thomasii* from shallow-water environments associated with hermatypic corals, with moderate to high hydrodynamic energy.

Together with *S. thomasii*, *T. pustulatum* is one of the most common and abundant coralline algae in the Uromieh section. Its presence in lower to middle Rupelian limestones (Figs 2, 9) is important for coralline algae stratigraphy since it is the earliest occurrence of the species known so far. According to Bassi et al. (2009) the oldest-known record of *T. pustulatum* is from the upper Oligocene shallow-water carbonates of the Kōko Seamount in Central Pacific. Based on this, the authors suggest the Pacific Ocean as spreading center for *T. pustulatum* (Bassi et al. 2009, as *Lithophyllum pustulatum*). However, the specimens of Uromieh move the oldest record of the species into the Rupelian Tethys, and suggest that the paleobiogeography of this species, so common and abundant in modern oceans, is still insufficiently known.

Conclusions

The Uromieh section of the Qom Formation is characterized by abundant corals (mostly colonial), porcellanaceous foraminifera (both large and small), large rotaliids, and coralline algae (both crustose and articulated). Their distribution is not uniform, as they form several facies across the section. Echinoids and bryozoans are present but less common. Mollusks, green calcareous algae and serpulids are rare. The presence of *Nummulites fichteli*, *Nummulites vascus*, *Halkyardia maxima* and *Subterraniphyllum thomasii*, together with the absence of both *Nephrolepidina* and *Eulepidina*, suggest an early to middle Rupelian age for the investigated samples. The presence of a late Rupelian planktonic foraminiferal assemblage in the overlying marls support this hypothesis.

In the lower part of the section, the abundance of miliolids and corals suggests a proximal inner-platform environment. Toward the upper part of the section, the increase in large rotaliids,

coralline algae and bryozoans points toward a distal inner-platform or proximal middle-platform setting. The coralline algal assemblages support this paleoenvironmental interpretation.

Crustose Corallinales and articulated coralline algae dominate the whole section, with *L. melobesioides*, *T. pustulatum* and *S. thomasii* beeing the most common species. Sporolithales and Hapalidiales are more common in the upper part of the section.

S. thomasii is generally more common in coral-rich intervals, suggesting that this species has a preference toward shallow-water environments. The specimens of *T. pustulatum* recovered in the Uromieh section predate all the other known record of this species, indicating that *T. pustulatum* originated at least in the Rupelian, much earlier than previously thought.

This analysis suggests that there is still much to discover on the stratigraphy and the distribution of coralline algae. Even though this group is one of the most important carbonate producers of modern shelves, its evolutionary history is still incomplete and fragmentary.

References

Abaie I., Ansari H.J., Badakhshan A. & Jaafari A. (1964) - History and development of the Alborz and Sarajeh fields of Central Iran. *Bull. Iran. Petrol. Inst.*, 15: 561-574.

Adey W.H. (1979) - Crustose coralline algae as microenvironmental indicators in the Tertiary. In: Gray J. & Boucot A.J. (Eds) - Historical Biogeography, Plate Tectonics and the changing environment: 459-464. Proceedings of the thirty-seventh Annual Biology Colloquium.

Adey W.H. (1986) - Coralline algae as indicators of sea-level. In: Van de Plassche O. (Ed.) - Sea-level research: a manual for the collection and evaluation of data: 229-280. Geo-Books, Norwich.

Adey W.H & Macintyre I.G. (1973) - Crustose coralline algae: a re-evaluation in the geological sciences. *Geol. Soc. Am. Bull.*, 84: 883-904.

Adey W.H., Townsend R.A. & Boykins W.T. (1982) - The crustose coralline algae (Rhodophyta: Corallinaceae) of the Hawaiian Islands. Smithsonian contribution to Marine Sciences 15, 84 pp.

Agard P., Omrani, J., Jolivet L., Whitechurch H., Vrielynck B., Spakman W., Monié P., Meyer B. & Wortel R. (2011) - Zagros orogeny: a subduction-dominated process. *Geol. Mag.*, 148: 692-725.

Aguirre J., Braga J.C. & Bassi D. (2011) - Taxonomic assessment of coralline algal species (Rhodophyta; Corallinales and Sporolithales) described by Pfender, Lemoine and Miranda from Northern Spain type Localities. *Ann. Naturhist. Mus. Wien. Serie A*, 113: 267-289.

Baccelle L. & Bosellini A. (1965) - Diagrammi per la stima visiva della composizione percentuale nelle rocce sedimentarie. *Ann. Univ. Ferrara, Nuova Serie, Sezione IX, Sci. Geol. Paleontol.*, 1: 59-89.

Ballato P., Nowaczyk N.R., Landgraf A., Strecker M.R., Friedrich A. & Tabatabaei S.H. (2008) - Tectonic control on sedimentary facies pattern and sediment accumulation rates in the Miocene foreland basin of the southern Alborz mountains, northern Iran. *Tectonics,* 27, doi:10.1029/2008TC002278.

Bassi D. (1997) - Vegetative anatomy and palaeoecology of *Polystrata alba* (Pfender) Denizot, 1968 (Cryptonemiales, Peyssonneliaceae) from the upper Eocene of northern Italy. *Rev. Paleobiol.*, 16: 309-320.

Bassi D., Braga J.C. & Iryu Y. (2009) - Palaeobiogeographic patterns of a persistent monophyletic lineage: *Lithophyllum pustulatum* species group (Corallinaceae, Corallinales, Rhodophyta). *Palaegeogr., Palaeoclimatol., Palaeoecol.*, 284: 237-245.

Bassi D., Braga J. C., Zakrevskaya E. & Petrovna Radionova E. (2007) - Redescription of the type collections of Maslov's species of Corallinales (Rhodophyta). II. Species included by Maslov in *Archaeolithothamnium* Rothpletz, 1891. *Rev. Esp. Paleontol.*, 22(2): 115-125.

Bassi D. & Nebelsick J.H. (2000) - Calcareous algae from the lower Oligocene Gornji Grad beds of Northern Slovenia. *Riv. It. Paleont. Strat.*, 106: 99-122.

Bassi D., Woelkerling W.J. & Nebelsick J.H. (2000) - Taxonomic and biostratigraphical re-assessments of *Subterraniphyllum* Elliott (Corallinales, Rhodophyta). *Palaeontology*, 43: 405-425.

Basso D. (1995) - Living calcareous algae by a paleontological approach: the genus *Lithothamnion* Heydrich nom. cons. from the soft bottoms of the Tyrrhenian Sea (Mediterranean). *Riv. It. Paleont. Strat.,* 101: 349-366.

Basso D. (2012) - Carbonate production by calcareous red algae and global change. In: Basso D. & Granier B. (Eds) - Calcareous algae and global change: from identification to quantification. *Geodiversitas*, 34: 13-33.

Basso D., Fravega P. & Vannucci G. (1996) - Fossil and living corallinaceans related to the Mediterranean endemic species *Lithophyllum racemus* (Lamark) Foslie. *Facies*, 35: 275-292.

Basso D., Morbioli C. & Corselli C. (2006) - Rhodolith facies evolution and burial as response to Holocene transgression at the Pontian Islands shelf break. In: Pedley H.M. & Carannante G. (Eds) - Cool-water carbonates: depositional systems and palaeoenvironmental control. *Geol.*

Soc. London, Spec. Publ., 255: 23-34.

Basso D., Nalin R. & Nelson C.S. (2009) - Shallow-water *Sporolithon* rhodoliths from North Island (New Zealand). *Palaios*, 24: 92-103.

Benzoni F., Basso D., Caragnano A. & Rodondi G. (2011) - *Hydrolithon* spp. (Rhodophyta, Corallinales) overgrow live corals (Cnidaria, Scleractinia) in Yemen. *Mar Biol.*, DOI 10.1007/s00227-011-1743-2.

Berberian M. & King G. (1981) - Towards a paleogeography and tectonic evolution of Iran. *Canad. J. Earth Sci.*, 18: 210-265.

Bina M.M., Bucur I., Prevot M., Meyerfeld Y., Daly L., Cantagrel J.M. & Mergoil J. (1986) - Palaeomagnetism, petrology and geochronology of Tertiary magmatic and sedimentary units from Iran. *Tectonophysics*, 121: 303-329.

Bourrouilh Le Jan F.G. & Hottinger L.C. (1988) - Occurrence of rhodoliths in the tropical Pacific - a consequence of Mid-Miocene paleo-oceanographic change. *Sedim. Geol.*, 60: 355-367.

Bozorgnia F. (1965) - Qum Formation stratigraphy of the Central Basin of Iran and its intercontinental position. *Bull. Iran. Pet. Inst.*, 24: 69-75.

Braga J.C. & Aguirre J. (2001) - Coralline algal assemblages in Upper Neogene reef and temperate carbonates in Southern Spain. *Palaegeogr., Palaeoclimatol., Palaeoecol.*, 175: 37-41.

Braga J.C. & Bassi D. (2007) - Neogene history of *Sporolithon* Heydrich (Corallinales, Rhodophyta) in the Mediterranean region. *Palaegeogr., Palaeoclimatol., Palaeoecol.*, 243: 189-203.

Braga J.C., Bassi D. & Piller W.E. (2010) - Paleoenvironmental significance of Oligocene-Miocene coralline red algae - a review. In: Mutti M., Piller W.E. & Betzler C. (Eds) - Carbonate system during the Oligocene-Miocene Climatic Transition. *Int. Assoc. Sedimentol. Spec. Publ.*, 42: 165-182.

Braga J.C., Bosence D.W.J. & Steneck R.S. (1993) - New anatomical characters in fossil coralline algae and their taxonomic implications. *Palaeontology*, 36: 535-547.

Braga J.C., Vescogni A., Bosellini F.R. & Aguirre J. (2009) - Coralline algae (Corallinales, Rhodophyta) in the western and central Mediterranean Messinian reefs. *Palaegeogr., Palaeoclimatol., Palaeoecol.*, 275: 113-128.

Brandano M., Frezza V., Tomassetti L, Pedley M. & Matteucci R. (2009) - Facies analysis and paleoenvironmental interpretaton of the late Oligocene Attard Member (Lower Coralline Limestone Formation), Malta. *Sedimentology*, 56: 1138-1158.

Brandano M., Morsili M., Vannucci G., Parente M., Bosellini F. & Mateau-Vicens G. (2010) - Rhodolith-rich lithofacies of the Porto Badisco Calcarenites (upper Chattian, Salento, Southern Italy). *It. J. Geosci.,* 129: 119-131.

Cahuzac B. & Poignant A. (1997) - An attempt of biozonation of the Oligo-Miocene in the European basins, by means of larger neritic foraminifera. *Bull. Soc. Geol. France*, 168: 155-169.

Caragnano A., Basso D. & Rodondi G. (2016) - Growth rates and ecology of coralline rhodoliths from the Ras Ghamila back reef lagoon, Red Sea. *Mar. Ecol.*, 37: 713-726.

Caragnano A., Foetisch A., Maneveldt G.W., Millet L., Liu L-C, Lin S-M, Rodondi G. & Payri C.E. (2018) - Revision of Corallinaceae (Corallinales, Rhodophyta): recognizing *Dawsoniolithon* gen. nov., *Parvicellularium* gen. nov. and Chamberlainoideae subfam. nov. containing *Chamberlainium* gen. nov. and *Pneophyllum. J. Phycol.,* 54, doi:10.1111/jpy.12644.

Chamberlain Y.M. & Irvine L.M. (1994) - Lithophylloideae Setchell. In: Irvine L.M. & Chamberlain Y.M. (Eds) - Seaweeds of the British Isles, Volume 1 Rhodophyta Part 2B Corallinales, Hildenbrandiales: 58-112. HMSO, London.

Chelaru R. & Bucur I. (2016) - The taxonomy of middle Miocene red algae from the Gârbova de Sus Formation (Transylvanian Basin, Romania). *Carnets Geol.*, 16: 307-336.

Coletti G. (2016) - Nutrients influence on Miocene carbonate factories. PhD Thesis, unpubl. Univ. degli Studi di Milano-Bicocca.

Coletti G., Basso D. & Corselli C. (2018) - Coralline algae as depth indicators in the Sommières Basin (early Miocene, Southern France). *Geobios*, 51: 15-30.

Coletti G., Basso D. & Frixa A. (2017) - Economic importance of coralline carbonates. In: Riosmena-Rodriguez R., Nelson W. & Aguirre J. (Eds) - Rhodolith/Maerl beds: a global perspective. Coastal Research Library 15: 87-101, Springer-Verlag, Berlin.

Coletti G., Vezzoli G., Di Capua A. & Basso D. (2016) - Reconstruction of a lost carbonate factory based on its biogenic detritus (Ternate-Travedona and Gonfolite Lombarda Group - Northern Italy). *Riv. It. Paleont. Strat.*, 122: 1-22.

Davoudian A.R., Genser J., Neubauer F. & Shabanian N. (2016) - ^{40}Ar/^{39}Ar mineral ages of eclogites from North Shahrekord in the Sanandaj-Sirjan Zone, Iran: Implications for the tectonic evolution of Zagros orogen. *Gondwana Res.*, 37: 216-240.

Denizot M. (1968) - Les algues floridées encroutantes (à l'éxclusion des Corallinacées). Paris, Laboratoire de Cryptogamie, Muséum National d'Histoire Naturelle, 310 pp.

Elliott G. F. (1957) - *Subterraniphyllum*, a new Tertiary calcareous alga. *Palaeontology*, 1: 73-75.

Flügel E. (2010) - Microfacies of Carbonate Rocks: Analysis Interpretation and Application. Springer, New York, 984 pp.

Fravega P., Piazza M. & Vannucci G. (1993) - Three new species of coralline algae (genera *Lithothamnion* and *Lithophyllum*) from the Tertiary Piedmont Basin. *Riv. It. Paleont. Strat.,* 4: 453-466.

Furrer M. & Soder P. (1955) - The Oligo-Miocene marine formation in the Qom region (Central Iran), Proceedings of the 4th World Petroleum Congress, Rome, Section I/A/5, 267-277.

Gale L. (2009) - Non-geniculate coralline algae (Corallinales, Rhodophyta) from the lower Oligocene of Polšica Pri

Podnartu (Nothern Slovenia). *Riv. It. Paleont. Strat.,* 115: 87-100.

Gansser A. (1955) - New aspects of the Geology in Central Iran (Iran), 4th World Petroleum Congress, Section I/A/ 5, paper 2 Rome: 279-300.

Guiry M.D. & Guiry G.M. (2019) - AlgaeBase. World-wide electronic publication, National University of Ireland, Galway. http://www.algaebase.org; searched on 02 February 2019.

Halfar J. & Mutti M. (2005) - Global dominance of coralline red-algal facies: a response to Miocene oceanographic events. *Geology*, 33(6): 481-484.

Harvey A.S., Broadwater S.T., Woelkerling W.J. & Mitrovski P.J. (2003) - *Choreonema* (Corallinales, Rhodophyta): 18S rDNA phylogeny and resurrection of the Hapalidiaceae for the subfamilies Choreonematoideae, Austrolithoideae, and Melobesioideae. *J. Phycol.,* 39: 988-998.

Harvey A.S., Phillips L.E., Woelkerling W.J. & Millar A.J.K. (2006) - The Corallinaceae, subfamily Mastophoroideae (Corallinales, Rhodophyta) in south-eastern Australia. *Australian System. Bot.,* 19: 387-429.

Harvey A.S., Woelkerling W.J. & Millar A.J.K. (2009) - The genus *Lithophyllum* (Lithophylloideae, Corallinaceae, Rhodophyta) in south-eastern Australia, with the description of *L. riosmenae*, sp. nov. *Australian System. Bot.,* 22: 296-317.

Hassanzadeh J. & Wernicke B.P. (2016) - The Neotethyan Sanandaj-Sirjan zone of Iran as anarchetype for passive margin-arc transitions. *Tectonics*, 35: 586-621.

Hernandez-Kantun J.J., Gabrielson P.W., Hughey J.R., Pezzolesi L., Rindi F., Robinson N.M., Peña V., Riosmena-Rodriguez R.Le., Gall L. & Adey W.H. (2016) - Reassessment of branched *Lithophyllum* spp. (Corallinales, Rhodophyta) in the Caribbean Sea with global implications. *Phycologia,* 55: 609-35.

Hottinger L. (2007) - Revision of the foraminiferal genus *Globoreticulina* Rahaghi, 1978, and its associated fauna of larger foraminifera from the late Middle Eocene of Iran. *Carnet de Géologie / Notebooks on Geology*, GG 2007-A06: 1-51.

Hottinger L., Halicz E. & Reiss Z. (1991) - The foraminiferal genera *Pararotalia*, *Neorotalia* and *Calcarina*, taxonomic revision. *J. Paleontol.*, 65: 18-33.

Hrabovský J., Basso D. & Doláková N. (2015) - Diagnostic characters in fossil coralline algae (Corallinophycidae: Rhodophyta) from the Miocene of southern Moravia (Carpathian Foredeep, Czech Republic). *J. Syst. Paleontol.*, 14: 499-525.

Johansen H.W. (1981) - Coralline Algae: A First Synthesis. CRC Press, Boca Raton, Florida, 239 pp.

Johnson J.H. (1966) - 1966. Tertiary red algae from Borneo. *Bull. British Mus. (Nat. Hist.), Geol. Ser.*, 2: 257-280.

Jones R.W. & Racey A. (1994) - Cenozoic stratigraphy of the Arabian Peninsula and Gulf. In: Simmons M.D. (Ed.) - Micropalaeontology and Hydrocarbon Exploration in the Middle East: 273-307. Chapman & Hall, UK.

Kato A., Baba M., Kawai H. & Masuda M. (2006) - Reassessment of the little-known crustose red algal genus

Polystrata (Gigartinales), based on morphology and ssu rdna sequences. *J. Phycol.*, 42: 922-933.

Keats D.W., Maneveldt G.W., Baba M., Chamberlain Y.M. & Lewis J.E. (2009) - Three species of *Mastophora* (Rhodophyta: Corallinales, Corallinaceae) in the tropical Indo-Pacific Ocean: *M. rosea* (C. Agardh) Setchell, *M. pacifica* (Heydrich) Foslie, and *M. multistrata* sp. nov. *Phycologia*, 48: 404-422.

Le Gall L., Payri C., Bittner L. & Saunders G.W. (2009) - Multigene polygenetic analyses support recognition of the Sporolithales, ord. nov. *Molec. Phylogen. Evol.,* 54: 302-305.

Lemoine M. (1977) - Étude d'une collection d'Algues Corallinacées de la région de Skopje (Yougoslavie). *Rev. Micropaléontol.*, 20: 10-43.

Letouzey J. & Rudkiewicz J. (2005) - Structural geology in the Central Iranian Basin. Institut Français du Pétrole, Rep. F0214001, 79 pp.

Loeblich A.R. & Tappan H. (1987) - Foraminiferal Genera and Their Classification. Van Nostrand Reinhold, New York, 1820 pp.

Lund M., Davies, P.J. & Braga J.C. (2000) - Coralline algal nodules off Fraser Island, Eastern Australia. *Facies*, 42: 25-34.

Maneveldt G.W., Gabrielson P.W. & Kangwe J. (2017) - *Sporolithon indopacificum* sp. nov. (Sporolithales, Rhodophyta) from tropical western Indian and western Pacific oceans: first report, confirmed by DNA sequence data, of a widely distributed species of *Sporolithon*. *Phytotaxa*, 326: 115-128.

Mastrorilli V.I. (1968) - Caratteri morfologici e strutturali di un esemplare fertile di "*Subterraniphyllum*" Elliot rinvenuto nell'Oligocene di Ponzone. *Riv. It. Paleont. Strat.,* 74: 1275-1288.

Mattei M., Cifelli F., Muttoni G., Zanchi A., Berra F., Mossavvari F. & Eshraghi S.A. (2012) - Neogene block rotation in central Iran: evidence from paleomagnetic data. *GSA Bull.*, 124: 943-956.

Minnery G.A., Rezak R. & Bright T.J. (1985) - Depth zonation and growth form of crustose coralline algae: Flower Garden Banks, Northwestern Gulf of Mexico. In: Toomey D.F. & Nitecki, M.H. (Eds) - Paleoalgology: Contemporary Research and Applications: 237-246. Springer, New York.

Mastrorilli V.I. (1968) - Caratteri morfologici e strutturali di un esemplare fertile di *Subterraniphyllum* Elliott rinvenuto nell'Oligocene di Ponzone (Piemonte). *Riv. It. Paleont. Strat.,* 74: 1275-1283.

Misra P.K., Jauhri A.K., Singh S.K. & Kishore S. (2001) - Coralline Algae from the Oligocene & Eocene of Kachchh, Gujarat, India. *J. Palaeontol. Soc. India*, 46: 59-76.

Mohammadi E., Hasanzadeh-Dastgerdi M., Ghaedi M., Dehghan R., Safari A., Vaziri-Moghaddam H., Baizidi C., Vaziri M.R. & Sfidari E. (2013) - The Tethyan Seaway Iranian Plate Oligo-Miocene deposits (the Qom Formation): distribution of Rupelian (Early Oligocene) and evaporate deposits as evidences for timing and trending of opening and closure of the Tethyan Seaway. *Carb. Evap.*, 28: 321-345.

Mohammadi E., Vaziri M.R. & Dastanpour M. (2015) - Biostratigraphy of the nummulitids and lepidocyclinids bearing Qom Formation based on larger benthic foraminifera (Sanandaj-Sirjan fore-arc basin and Central Iran back-arc basin, Iran). *Arab. J. Geosci.*, 8: 403-423.

Montaggioni L.F., Behairy A.K.A., El-Sayed M.K. & Yusuf N. (1986) - The modern reef complex, Jeddah area, Red Sea: a facies model for carbonate sedimentation on embryonic passive margins. *Coral Reefs,* 5: 127-150.

Morley C.K., Julapour A.A., Abdolghafourian M., Hajian M., Waples D., Warren J., Otterdoom H., Srisuriyon K. & Kazemi H. (2009) - Structural development of a major late Cenozoic basin and transpressional belt in central Iran: The Central Basin in the Qom-Saveh area. *Geosphere,* 5: 325-362.

Nebelsick J.H., Bassi D. & Lempp J. (2013) - Tracking paleoenvironmental changes in coralline algal-dominated carbonates of the Lower Oligocene Calcareniti di Castelgomberto Formation (Monti Berici, Italy). *Facies,* 59: 133-148.

Nebelsick J.H., Rasser M.W. & Bassi D. (2005) - Facies dynamics in Eocene to Oligocene circumalpine carbonates. *Facies*, 51: 197-216.

Nelson W.A., Sutherland J.E., Farr T.J., Hart D.R., Neill K.F., Kim H.J. & Yoon H.S. (2015) - Multi-gene phylogenetic analyses of New Zealand coralline algae *Corallinapetra novaezelandiae* gen. et sp. nov. and recognition of the Hapalidiales ord. nov. *J. Phycol.*, 51: 454-468.

Penrose D.L. (1996) - Genus *Hydrolithon* (Foslie) Foslie 1909. In: Womersley, H.B.S. (Ed.) - The Marine Benthic Flora of South Australia. Rhodophyta. Part III, Gracilariales, Rhodymeniales, pp. 273-280. Canberra: Australian Biological Resources Study.

Perrin C., Bosence D.W.J. & Rosen B. (1995) - Quantitative approaches to palaeozonation and palaeobathymetry of corals and coralline algae in Cenozoic reefs. In: Bosence D.W.J. & Allison P.A. (Eds) - Marine Palaeoenvironmental Analysis from Fossils. *Geol. Soc. Spec. Pub.,* 83: 181-229.

Pezzolesi L., Peña V., Le Gall L., Gabrielson P.W., Kaleb S., Hughey J.R., Rodondi G., Hernandez-Kantun J.J., Falace A., Basso D., Cerrano C. & Rindi F. (2019) - Mediterranean *Lithophyllum stictiforme* (Corallinales, Rhodophyta) is a genetically diverse species complex: implications for species circumscription, biogeography and conservation of coralligenous habitats. DOI: 10.1111/jpy.12837 (Electronic publication ahead of print).

Poignant A.F. (1985) - Présentation simplifiée d'une nouvelle classification générique des Rhodophycées mésozoïques et cénozooïques. Informatisation. *Bull. Soc. Géol. France* 8: 603-605.

Pomar L., Baceta J., Hallock P., Mateu-Vicens G. & Basso D. (2017) - Reef building and carbonate production modes in the west-central Tethys during the Cenozoic. *Mar. Pet. Geol.*, doi: 10.1016/j.marpetgeo.2017.03.015.

Pomar L., Mateu E., Martinez W., Espino D., Castillo de Ott V., Benkovics L. & Castro Leyva T. (2015) - Oligocene-Miocene carbonates of the Perla field, offshore Venezuela:

Depositional model and facies architecture. In: Bartolini C. & Mann P. (Eds) - Petroleum geology and potential of the Colombian Caribbean Margin. *AAPG Memoir,* 108: 647-674.

Quaranta F., Tomassetti L., Vannucci G. & Brandano M. (2012) - Coralline algae as environmental indicators: a case study from the Attard member (Chattian, Malta). *Geodiversitas*, 34: 151-166.

Quaranta F., Vannucci G. & Basso D. (2007) - *Neogoniolithon contii* comb. nov. based on the taxonomic re-assessment of Mastrorilli's original material from the Oligocene of NW Italy (TPB). *Riv. It. Paleont. Strat.,* 113: 43-55.

Racey A. (1994) - Biostratigraphy and palaeobiogeographic significance of Tertiary nummulitids (foraminifera) from northern Oman. In: Simmons M.D. (Ed.) - Micropalaeontology and Hydrocarbon Exploration in the Middle East: 343-367. Chapman & Hall, UK.

Rasser M.W. (2001) - Paleoecology and taphonomy of *Polystrata alba* (red alga) from the Late Eocene Alpine Foreland: a new tool for the reconstruction of sedimentary environments. *Palaios,* 16: 601-607.

Reuter M., Piller W., Harzhauser M., Mandic O., Berning B., Rögl F., Kroh A., Aubry M.-P., Wielandt-Schuster U. & Hamedani A. (2009) - The Oligo-/Miocene Qom Formation (Iran): evidence for an early Burdigalian restriction of the Tethyan Seaway and closure of its Iranian gateways. *Intern. J. Earth Sci.*, 98: 627-650.

Richards & Fredericq (2018) - *Sporolithon sinusmexicanum* sp. nov. (Sporolithales, Rhodophyta): a new rhodolith-forming species from deepwater rhodolith beds in the Gulf of Mexico. *Phytotaxa,* 350(2): 135-146.

Riosmena-Rodríguez R. (2017) - Natural History of Rhodolith/Maërl Beds: Their role in near-shore biodiversity and management. In: Riosmena-Rodríguez R., Nelson W. & Aguirre J. (Eds) - Rhodolith/Maërl Beds: A Global Perspective, 15: 3-27. Springer, Coastal Research Library.

Rösler A., Perfectti F., Peña V. & Braga J.C. (2016) - Phylogenetic relationships of Corallinaceae (Corallinales, Rhodophyta): taxonomic implications for reef-building corallines. *J. Phycol.*, 52: 412-431.

Sanfilippo R., Rosso A., Basso D., Violanti D., Di Geronimo I., Di Geronimo R., Benzoni F. & Robba E. (2011) - Cobbles colonization pattern from a tsunami-affected coastal area (SW Thailand, Andaman Sea). *Facies*, 57: 1-13.

Sartorio D. & Venturini S. (1988) - Southern Tethys Biofacies. Agip S.p.A., Milano, 235 pp.

Sattler U, Zampetti V, Schlager W. & Immenhauser A. (2004) - Late leaching under deep burial conditions: a case of study from the Miocene Zhujiang Carbonate Reservoir, South China Sea. *Mar. Pet. Geol.,* 21: 977-992.

Spezzaferri S. (1994) - Planktonic foraminiferal biostratigraphy and taxonomy of the Oligocene and Lower Miocene in the oceanic record. An overview. *Paleontographica Italica*, 81: 1-187.

Stöcklin J. (1968) - Structural history and tectonics of Iran: a review. *AAPG Bull.*, 52: 1229-1258.

Stöcklin J. & Nabavi M. (1973) - Tectonic map of Iran

(1:2,500,000). Geological Survey of Iran, Tehran.

Vadas R.L. & Steneck R.S. (1988) - Zonation of deep water benthic algae in the Gulf of Maine. *J. Phycol.,* 24: 338-346.

Van der Merwe E. & Maneveldt G.W. (2015) - A modern account of the South African non-geniculate Lithophylloideae (Corallinales, Corallinophycidae, Rhodophyta). *South Afr. J. Bot.,* 103: 247-267.

Vannucci G., Basso D. & Fravega P. (2000b) - New observations on the anatomy of *Subterraniphyllum* Elliot. *Riv. It. Paleont. Strat.,* 106: 237-246.

Vannucci G., Piazza M., Fravega P. & Basso D. (2000a) - Revision and re-documentation of Airoldi's species of *Archaeolithothamnium* from the Tertiary Piedmont Basin (NW Italy). *Riv. It. Paleont. Strat.,* 106: 191-202.

Vannucci G., Quaranta F. & Basso D. (2008) - Revision and re-documentation of M. Airoldi species of *Lithophyllum* from the Tertiary Piedmont Basin. *Riv. It. Paleont. Strat.,* 114: 515-528.

Vannucci G., Quaranta F. & Basso D. (2010a) - Revision and re-documentation of M. Airoldi species of *Lithothamnion* from the Tertiary Piedmont Basin. *Riv. It. Paleont. Strat.,* 116: 223-235.

Vannucci G., Testa M., Piazza M. & Pastorino P. (2010b) - *Subterranyphyllum* and free-living *Neogoniolithon* from the Oligocene reef facies of Costa d'Ovada (Tertiary Piedmont Basin, Alessandria, NW Italy). *It. J. Geosci.,* 129: 4-14.

Vaziri-Moghaddam H., Kimiagari M. & Taheri A. (2006) - Depositional environment and sequence stratigraphy of the Oligo-Miocene Asmari Formation in SW Iran. *Facies,* 52: 41-51.

Verheij E. (1993) - The genus *Sporolithon* (Sporolithaceae fam. nov., Corallinales, Rhodophyta) from the Spermonde Archipelago, Indonesia. *Phycologia,* 32: 184-196.

Wade B.S., Pearson P.N., Berggren W.A. & Pälike H. (2011) - Review and revision of Cenozoic tropical planktonic foraminiferal biostratigraphy and calibration to the geomagnetic polarity and astronomical time scale. *Earth Sci. Rev.,* 104: 111-142.

Woelkerling W.J. (1988) - The coralline red algae: an analysis of the genera and subfamilies of nongeniculate Corallinaceae. Oxford University Press, New York, 268 pp.

Woelkerling W.J., Irvine L.M. & Harvey A.S. (1993) - Growth-forms in non-geniculate coralline red algae (Corallinales Rhodophyta). *Australian Syst. Bot.,* 6: 277-293.

Yazdi-Moghadam M. (2011) - Early Oligocene larger foraminiferal biostratigraphy of the Qom Formation, South Uromieh (NW Iran). *Turkish J. Earth Sci.,* 20: 847-856.

Yazdi-Moghadam M., Sadeghi A., Adabi M.H. & Tahmasbi A.R. (2018) - Foraminiferal biostratigraphy of the lower Miocene Hamzian and Arashtanab sections (NW Iran), northern margin of the Tethyan Seaway. *Geobios,* 51: 231-246.

Zanchetta S., Berra F., Zanchi A., Bergomi M., Caridroit M., Nicora A. & Heidarzadeh G. (2013) - The record of the Late Palaeozoic active margin of the palaeotethys in NE Iran: Constraints on Cimmerian orogeny. *Gondwana Res.,* 24: 1237-1266.

Zanchetta S., Malaspina N., Zanchi A., Benciolini L., Martin S., Javadi H.R. & Kouhpeyma M. (2018) - Contrasting subduction-exhumation paths in the blueschists of the Anarak metamorphic complex (Central Iran). *Geol. Mag.,* 155: 316-334.

Zanchi A., Zanchetta S., Balini M. & Ghassemi M.R. (2016) - Oblique convergence during the Cimmerian collision: Evidence from the Triassic Aghdarband Basin, NE Iran. *Gondwana Res.,* 38: 149-170.

Zanchi A., Zanchetta S., Berra F., Mattei M., Garzanti E., Molyneux S., Nawab A. & Sabouri J. (2009) - The Eo-Cimmerian (Late? Triassic) orogeny in north Iran. *Geol. Soc. Spec. Publ.,* 312: 31-55.